DRUG LOADING AND RELEASE PROPERTIES OF MESOPOROUS SILICON NANOPARTICLES USING D-LUCIFERIN AS A DRUG-LIKE MODEL MOLECULE

Niko Kyllönen

Master of Science thesis

Programme of biosciences, major: biochemistry

University of Eastern Finland, Department of Health Sciences

January 2014

ABSTRACT

UNIVERSITY OF EASTERN FINLAND, Department of Health Sciences
Programme of Biosciences, major: Biochemistry
Niko Kyllönen: Drug loading and release properties of mesoporous silicon nanoparticles using D-luciferin as a drug-like model molecule
Master of Science thesis, 63 pages
Supervisors: PhD Ale Närvänen, PhD Pekka Poutiainen, MSc Jussi Rytkönen
January 2014

Keywords: porous silicon, nanoparticles, firefly luciferase, luciferin, drug delivery, imaging, small drugs

Mesoporous silicon is a form of silicon that has nano-sized holes (size 2 - 50 nm) in its structure. It can be used as a material for preparing nanoparticles (size less than 100 nm). The particles are non-toxic and have advantageous drug carrier properties. The porous surface provides a large surface area for drug delivery purposes. The surface can be modified to increase the resistance against degradation of the material. The surface chemistry of the particles and the properties of a drug as well as some external factors (for instance the composition of release medium) have an impact on both drug loading and release. The drug release can be rapid or, more preferably for targeted drug delivery, sustained. Furthermore, some surface modifications improve the migration of particles to desired targets including malfunctioning organs, inflamed tissues and tumor cells while the others allow the sustaining of the drug release until the particles end up in their destination.

The drug release properties of nanoparticles are often monitored by labeling the cargo and/or the carrier. Traditional methods include using radioactive and fluorescent labels. Moreover, non-labelling bioluminescence based methods have recently attracted attention due to their simplicity compared to the label-based methods. An interesting idea is using D-luciferin as a drug-like model molecule. D-luciferin is fluorescent, has drug-like properties and also serves as a substrate in a bioluminescence reaction catalyzed by luciferase.

In this study drug loading and release properties of mesoporous silicon nanoparticles were studied by using D-luciferin as a drug-like model molecule. D-luciferin was un-covalently loaded into three types of porous silicon particles. Fluorescence measurements were performed in order to compare drug loading properties of the particles. The most potent carrier candidate was loaded in order to carry out an enzymatic release study.

The results showed the highest loading capacity for thermally carbonized porous silicon nanoparticles. Unfortunately, these particles showed a rapid release of all of the loaded D-luciferin. On the other hand, methods used in the current study were realized to be useful for comparing drug release properties of different types of porous silicon nanoparticles. The loading and release study could be repeated with the same protocol using some other particles. Furthermore, the release medium requires optimization. Strong bioluminescence light provides prospects to use D-luciferin as a model drug/label for imaging drug delivery with luciferase transfected cells.

PROLOGUE

This Master's Thesis was done in the University of Eastern Finland in the Department of Health Sciences in Biomolecule Group between February 2013 and January 2014.

I would like to acknowledge my instructors Ale Närvänen, Jussi Rytkönen and Pekka Poutianen as well as Juha Pulkkinen (School of Pharmacy) for their guidance during the experimental part. Thanks to Joakim Riikonen (The Department of Applied Physics) for assisting me in writing the literary review. Thanks also to my colleagues at the School of Pharmacy for refreshing my mind during the breaks.

Special thanks to my girlfriend for encouraging me while ploughing through this Master's Thesis project.

ABBREVIATIONS

% w/w Drug loading degree ($m_{drug\ loaded}$ / ($m_{drug\ loaded}$ + $m_{particle}$)

AEAPMS 3-(2-aminoethylamino) propyldimethoxymethylsilane

AMP Adenosine monophosphate

BSA Bovine serum albumin fraction V

Chloramine T Tosylchloramide sodium

CPP Cell penetrating peptide

D-LH_2 D-luciferin

DLS Dynamic light scattering

DMSO Dimethylsulfoxide

DTT Dithiothreitol

EDTA Ethylenediaminetetraacetic acid

FLIC Luciferase-specific inhibitor compounds

FLuc Firefly luciferase

FTIR Fourier transform infrared spectroscopy

HPLC High pressure liquid chromatography

IODO-GEN 1,3,4,6-tetrachloro-3α,6α-diphenyl glycoluril

LBL Layer-by-layer self-assembly

MCM-41 Mobil Composition of Matter 41

MPS Mononuclear phagocyte system

O-PEG Oleyl-poly(ethylene glycol)

PBS Phosphate buffer saline

PEG Poly(ethylene glycol)

pK_a logP (log ($c_{octanol}$ / c_{water})

PP_i Pyrophoshpate

PSi Porous silicon

RO5 Lipinski's rule of five

SSA Specific surface area

TCPSi-NH_2 Amine treated thermally carbonized porous silicon particles

TEM Transmission electron microscopy

TG Thermogravimetry

UnTHCPSi Undecylenic acid treated thermally hydrocarbonized porous silicon

WOPSi-NH_2 Amine treated wet-oxidized porous silicon particles

XRD X-ray diffraction

ζ-potential Zeta potential

TABLE OF CONTENTS

Introduction

Nanomedicine is a multidisciplinary field of research where the interest is in using nanomaterials to the advancement of health. One area of nanomedicine is targeted drug delivery where the goal is to deliver medications to the diseased area of the body in a manner that accumulates the drug to that area. The material is processed to different sizes of particles to carry drug molecules. For targeted drug delivery the type of particles are called *nanoparticles*. Nanoparticles are often defined as particles with a diameter less than 100 nm in diameter (Royal Society, 2007). The surface of the nanoparticles is modified to increase the circulation time in the body, cell specific targeting and membrane permeability. The properties of nanoparticles for example in cells (Bimbo et al. 2010) and in the body (Rytkönen et al. 2012) can be studied by labelling the particles with a radioactive or fluorescent label. Alternatively, the labelling of the cargo enables to study the release of the cargo.

D-luciferin ((S)-2-(6-hydroxybenzothiazol-2-yl)-2-thiazoline-4-carboxylic acid; PubMed ID 24896524) is a potential alternative marker for nanoparticle research. D-luciferin (D-LH_2) is an optical stereoisomer of *luciferin* (LH_2) whose asymmetric atom is carbon 2 in the thiazoline-carboxylic acid moiety (Marques & Esteves da Silva, 2009, Seliger et al. 1961) (Fig. 1). With magnesium ion (Mg^{2+}) and adenosine-triphosphate (ATP) D-LH_2 serves as a substrate to *firefly luciferase* (FLuc) in a bioluminescence reaction resulting in emission of visible light. (Seliger et al. 1961) (Fig. 1)

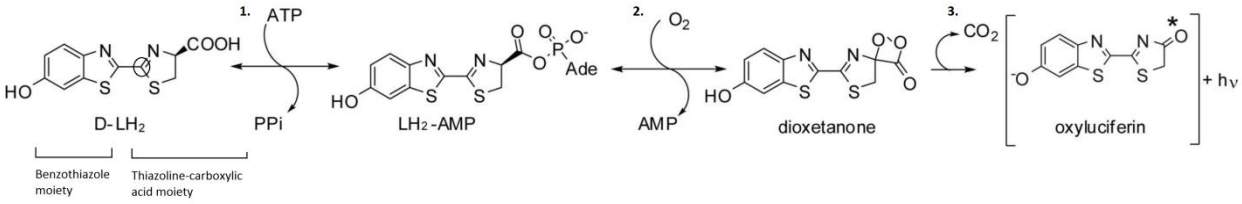

Figure 1. The luminescence reaction of D-luciferin (MW 280.32 g/mol) is a multistep process catalyzed by luciferase. The asymmetric carbon (circled) may change the structure to L-stereoisomer which does not react to emit yellow-green light. **(1)** In the first step, adenosine triphosphate (ATP) reacts with the carboxylic group of the thiazoline-carboxylic acid moiety of D-luciferin (D-LH_2). The hydrolysis of ATP produces pyrophosphate (PPi) and D-luciferyl-adenylate (LH_2-AMP), which may be induced by a bivalent cation (not shown). **(2)** In the second step molecular oxygen (O_2) replaces AMP forming dioxetanone. **(3)** Finally, carbon dioxide (CO_2) binds resulting oxyluciferin with an excited electron. Visible light (hv) is emitted for releasing the excitation state. (Modified from Marques & Esteves da Silva, 2009, Thorne et al. 2010)

The structure of D-LH_2 abides well the common drug-like properties (Lipinski et al. 1997, Lipinski, 2004) (Fig. 1). The size of D-LH_2 is small and it can be used as a model drug for nanoparticle loading and the release studies in FLuc containing environment. Traditionally, FLuc transfected cells are widely used in reporter gene assays are for imaging purposes (McElroy, 1951). The most notable advantage in using D-LH_2 as a model drug is to avoid the need for additional labeling which may affect the release of the cargo from nanoparticles as well as standard biological functions of cells. With this method one may also run a dual experiment to study both the release kinetics of D-LH_2 from nanoparticles and the transportation of traditionally labeled nanoparticles separately.

There are few publications dealing with combining D-LH_2 with porous silicon nanoparticles. For instance, Ding et al. (2012) introduced a method to study the effect of different nanoparticles to the Fluc transfected cells by loading D-LH_2 to the particles. Sun et al. (2011) showed mesoporous silicon nanoparticles can be used as a co-delivery system for enzymes and substrates in order to

control intracellular catalytic reactions. However, those studies do not focus on using D-LH_2 as a drug-like molecule for porous silicon mediated drug delivery.

In this report D-LH_2 was used as a model drug in order to test suitability of different porous silicon nanoparticles for drug loading and release for targeted drug delivery applications. In the first paragraph, porous silicon is introduced from the point of manufacturing and surface modifications. Furthermore, the principles of loading and release of small drugs using different types of porous silicon nanoparticles are discussed ending up comparison of the structural properties of D-LH_2 with recently loaded drug molecules (antipyrine, ibuprofen, griseofulvin, furosemide, ranitidine and indomethacin). In the end of the review some traditional radioactive and fluorescent labelling methods for nanoparticle research are introduced. Finally, in the experimental section D-LH_2 was loaded to three porous silicon nanoparticles with varying surface chemistries. The loading efficiency and the loading degree were determined by fluorescent spectroscopy. The release kinetics was studied using FLuc recombinant and measuring the luminescence light.

1. Literary review

2.1. The history of porous silicon - from optoelectronics to nanomedicine

Porous silicon (PSi) was accidentally manufactured during electropolishing of semiconductors for electronics industry in the 1950s (Uhlir, 1956). Instead of smooth corrosion the experiment resulted in the formation of pores on the surface of the substrate. The finding did not wake a remarkable interest until 1990 when prof. Canham reported the visible light emission after exciting PSi at room temperature by an external source of light. The discovery attracted attention in the optoelectronic industry (Torres-Costa et al. 2010) and also paved the way for the later progress of label-free imaging with luminescent nanoparticles (Park et al. 2009).

The crucial turning point in using PSi in medical applications took place when the pores of PSi were demonstrated to be linked to its bioactivity (Canham, 1996). In simulated body fluid PSi was shown to induce the growth of artificial hydroxyapatite, which, surprisingly, was dependent on the pores on the surface of PSi (Canham, 1996). The study not only inspired researchers to synthetize more functional PSi-based biomaterials for bone injuries (Canham, 2000, Low et al. 2006, Low et al. 2010) but also initiated engineering the material for other applications, for example PSi-based biosensors (Dhanekar & Jain, 2013, Mathew & Alocilja, 2003).

Some studies revealed that PSi could also be used as a safe material for drug delivery purposes. In 1998 Popplewell et al. carried out a study where silicon 32-isotope was administrated orally to a human subject. Mass spectroscopy measurements showed 90 % of the total gastrointestinal absorpted silicon was rapidly eliminated to non-toxic soluble orthosilic acid with a half-time of 2.7 hours. On the other hand, Anderson et al. (2003) showed the solubility in physiological conditions could be controlled by changing the porosity of a PSi layer.

Later many studies have presented methods how to increase the stability of PSi in the physiological conditions by modifying the surface chemistry of PSi. One of the very first positive demonstrations was carried out by Canham et al. (1999). In the study the stability of PSi layer in human blood plasma was dramatically increased after the surface of the silicon wafer was derivatized with 1-dodecyne. Several other studies have followed by variety of new stabilization methods against both oxidation and immunological responses from simple oxidation and carbonization methods (Bimbo et al. 2010, Limnell et al. 2007, Salonen et al. 2004, Wang et al. 2010) to complex linking of polymers (He et al. 2011, Passirani et al. 1998).

In 1992 a study by Mobil Corporation launched a technology to industrial catalytic purposes which could be used for receiving ordered silica sieves with hexagonal arrays of identical pores. One of their developed sieve type is called as *MCM-41* (**M**obil **C**omposition of **M**atter). The size of pores of MCM-41 varies between 2 and 50 nm defining a *mesoporous* material (Rouquerol et al. 1994). MCM-41 attracted attention as a potential platform for loading and sustaining the release of

poorly soluble drug molecules. In consequence, ibuprofen was the first model anti-inflammatory drug to be loaded into the pores of a MCM-41 wafer showing prolonged release in simulated body fluid (Vallet-Regi et al. 2001). The study gave evidence that morphologically similar silica pores can be used as ordered drug storing “pockets” without irreversible structural changes in the drug. Later some *in vitro* studies showed the loading and release properties are unavoidably dependent the physico-chemical properties of both a drug and the nanoparticles (Limnell et al. 2007, Salonen et al. 2005) indicating a requirement to perform separate loading and release tests for each drug carrier system.

Apart from taking advantage of nanoparticles as pharmacokinetic regulators there has been increased interest to use nanoparticles in targeting delivery of drugs to specific cells and tissues. Targeting would advance treatment of many obstinate diseases for example cancer therapy with cytostatic since most cytostatics are cytotoxic also for normal cells. Cytotoxicity for normal body cells may cause serious effects for example in the heart (Piasek et al. 2009). In fact, some interesting studies have recently come up regarding utilizing different biomolecules with specific cell transportation activities to increase the cell membrane permeability for several drug delivery systems (Hu et al. 2013, Kinnari et al. 2013, Park et al. 2005, Park et al. 2013). One example of those kind of biomolecules are *cell-penetrating peptides* (CPPs) which serve as ligands for endocytosis-inducing receptors expressed on the cell membrane (Arukuusk et al. 2013, Heitz et al. 2009, Mäe et al. 2009, Oskolkov et al. 2011). The first studies of combining CPPs with PSi nanoparticles have already been performed with promising results of improving *tumor homing* and even cell organelle specificity (Kinnari et al. 2013). The properties and applications of CPPs are described with more details elsewhere in the literature. Instead, in the current review we focus on the preparation and basic surface modification of non-specific delivery of PSi nanoparticles followed by discussion about what factors do actually affect the drug loading and release of small pharmaceuticals. Furthermore, different labelling methods for drug delivery are discussed.

2.2. Manufacturing and characterization

2.2.1. Classification of manufacturing methods of porous nanomaterials

Techniques for manufacturing of different types of porous nanomaterials can be divided to two main classes called *bottom-up* and *top-down* technologies which are based on contrary principles (Fig. 2). Bottom-up is based on using molecules and atoms as "building blocks" which are physico-chemically self-organized together to form a porous structure while top-down comprises reduction of a bulk material to nanoscale objects. (Raab et al. 2011) Bottom-up manufacturing techniques include an abundance of methods which can be further subcategorized into liquid phase and gas phase processes (Hofmeister et al. 1998, Li et al. 2004, Trewyn et al. 2007). The processes encompass for instance sol-gel (Trewyn et al. 2007), laser (Li et al. 2004), thermal and plasma-assisted processes (Hofmeister et al. 1998).

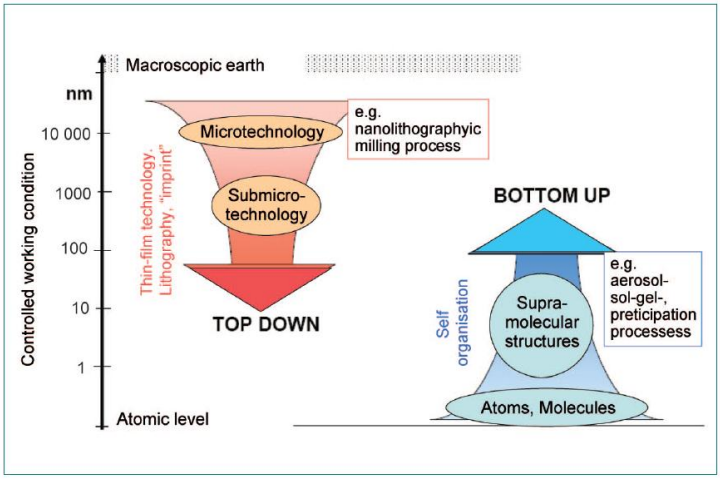

Figure 2. Two main technologies to produce porous nanomaterials differ from their starting point. The initial step of top-down techniques comprises for example a milling of a macro-sized material while bottom-up processes utilize the interactions between atoms and molecules. (Raab et al. 2011)

For drug delivery applications PSi nanoparticles are manufactured with top-down technology. The method is based on the original invention of Uhlir (1956). Briefly said, pores are directly etched to a solid layer in hydrofluoric acid solution (HF) either chemically with a strong oxidizing agent (for instance nitric acid) (Li et al. 2004, Vazsonyi et al. 2001) or electrochemically using an external electric field (Nychyporuk et al. 2006, Sailor, 2012, Salonen & Lehto, 2008, Trucks et al. 1990). Although some studies prefer to use oxidation techniques, electrochemical etching seems to stand the test of time as the most used method.

2.2.2. Electrochemical fabrication of porous silicon nanoparticles

Electrochemical etching can be performed with several types of equipment. The simplest system involves dipping two plates into the fabrication cell with a HF -solution (Fig. 3). The first plate is made of silicon and the other one is often platinum. The fabrication cell must be HF-resistance material, for instance Teflon. Switching the power supply on the etching begins as half reactions resulting etching of the silicon layer. (Salonen et al. 2008) One end product is hydrogen gas. Ethanol is added to improve the release of hydrogen bubbles from the pores and the external surface of the material. (Bley et al. 1996, Salonen et al. 2008)

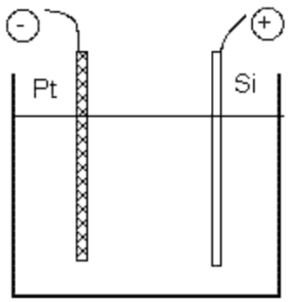

Figure 3. A comprehensive system for porous silicon etching. In the etching process the silicon layer is porosified whilst on the surface of non-corrosive platinum hydrogen is released. (Salonen, 2013)

For drug delivery, it is essential to achieve a high degree of pore homogeneity. The similarity of the pores is dependent on several parameters which may also be dependent on each other. These are for example an etching current (Asma et al. 2009, Nychyporuk et al. 2006), etching time, the composition of the electrolyte, (Bley et al. 1996) and even the presence of light (Kovalev, 2004). In addition, the type (phosphorus, n-type or boron, p-type) (Smith & Collins, 1990) and a proportion of the dopant (Yaakob et al. 2012) in the bulk silicon are extremely important factors affecting the success of the etching. A dopant gives a desired resistance to the pure silicon. The success of the etching can be seen in *transmission electron microscopy* (TEM) pictures (Smith & Collins, 1990) (Fig. 4). The etching mechanisms are complicated involving multiple breakings and formations of covalent bonds (Si-H, Si-F, Si-O, Si-Si) and are discussed carefully elsewhere (Sailor, 2012, Trucks et al. 1990).

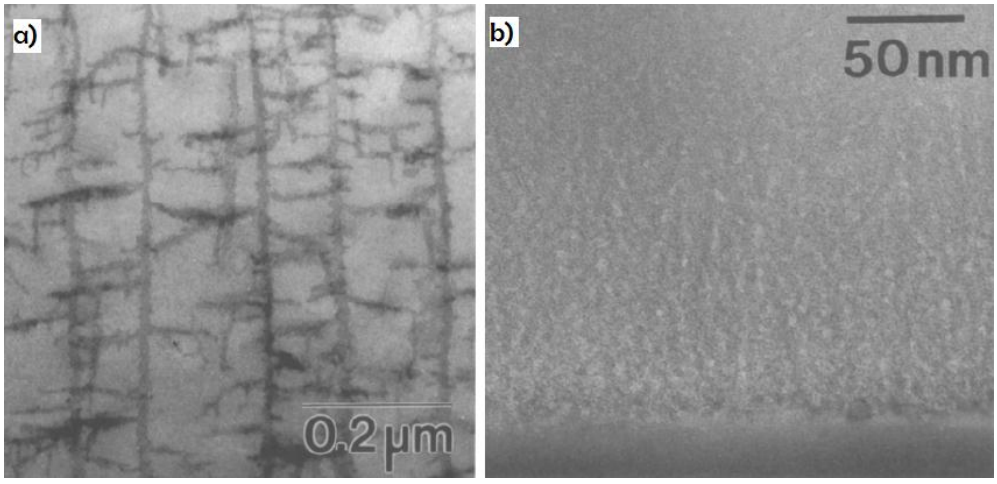

Figure 4. Cross-sectional transmission electron microscopy pictures of the porous silicon morphologies after anodizing in 10 % hydrofluoric acid at the current density 10 mA/cm^2. **a)** n-type porous silicon. **b)** p-type porous silicon. (Smith & Collins, 1990)

2.2.3. Drying and fragmentation of porous silicon films

Mechanical fragmentation of the etched PSi films is crucial in order to achieve a nanopowder appearance for PSi material. The fragmentation is usually carried out by *ultrasonic dispersion* (Bley et al. 1996, Kale, 2010, Park et al. 2009) or *ball-milling* (Bimbo et al. 2010, De Castro & Mitchell, 2002, Heintz et al. 2008, Kovalainen et al. 2012, Russo et al. 2012). An ethanol-based medium decreases the surface tension preventing the evaporation of the liquid from the pores (Björkqvist et al. 2003). The size distribution of the particles is studied by using a *dynamic light scattering* (DLS) or TEM instrument. (Bimbo et al. 2010, Rytkönen et al. 2012)

The fragmentation technique needs to be chosen according to the application where the particles are utilized. Ultrasonication is based on using high-frequency sound waves (> 20 kHz) to agitate a liquid sample (Royal Society of Chemistry 2013). It is effective especially for producing mono-dispersed luminescent nanoparticles (2 - 10 nm in diameter) for optical devices (Bley et al. 1996, Kale, 2010) and label-free imaging applications (Park et al. 2009). Instead, milling with ceramic balls is more used for producing drug carriers (Bimbo et al. 2010, Kovalainen et al. 2012, Rytkönen et al. 2012, Salonen et al. 2005). Milling results a wide particle-size range (Raab et al. 2011) but an extremely accurate particle size is required mainly in studies dealing with luminescence properties of nanoparticles.

Although fragmentation is a simple step in the nanoparticle fabrication, it still requires optimization. The size of particles and their pore morphology are not only important factors for determining the surface area for drug loading (Limnell et al. 2007) but have also other effects. For instance, cellular internalization (Huang & Chen, 2011) and *in vivo* biodistribution are dependent on the outer appearance of the PSi particles (He et al. 2011).

2.2.4. Stabilization against oxidative and chemical decomposition

It is well known that PSi is instabiel in ambient conditions and used to oxidize spontaneously over time. The reason is the oxidation of silicon hydrides (Si-H_x) on the PSi surface. (Canham et al. 1991, James et al. 2006) The oxidation has severe consequences. Firstly, the oxidized silicon particles have been noticed to degrade easily in a basic water solution, which sets boundaries to the utilization of PSi particles in drug delivery applications (Björkqvist et al. 2003). Secondly, the oxidation of PSi increases remarkably the hydrophilic nature of the PSi surface having an influence on the loading and the release of the cargo (Limnell et al. 2007). In the worst case, unnoticeable changes in the surface chemistry affect the reliability of results from experiments performed with differently aged PSi samples (Björkqvist et al. 2003, Salonen et al. 2005).

There are various stabilization methods including surface oxidation (Salonen et al. 2005, Salonen et al. 2008, Wang et al. 2010) and hydrocarbonization methods (Fig. 5) (Bimbo et al. 2010, Heintz et al. 2008, Kovalainen et al. 2012, Salonen et al. 2005, Salonen et al. 2008, Xia et al. 2005). Some studies propose more uncommon techniques for example rapid-thermal-oxidation of PSi layer performed after the etching process (Petrova-Koch et al. 1992). However, the immediate post-stabilization after the milling step is more common. The success of the stabilization can be studied by analyzing the spectra received from *Fourier transform infrared spectroscopy* (FTIR) (Chen et al. 1996, Limnell et al. 2007, Salonen et al. 2004, Xia et al. 2005) or measuring the weight increase in the particles (Salonen et al. 2004). The effect of the stabilization to the pore size should also be considered when designing a stable platform for a drug delivery application (Salonen et al. 2005).

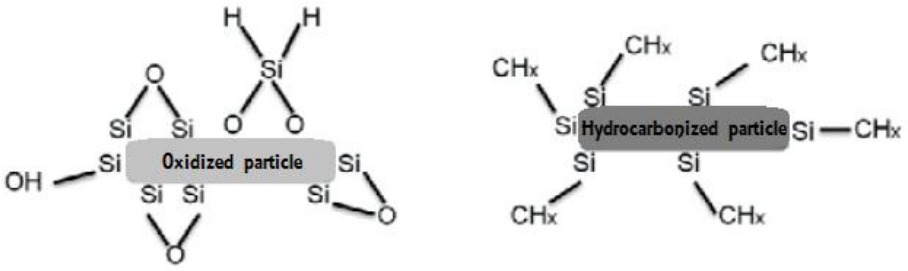

Figure 5. Porous silicon nanoparticles can be stabilized either by surface oxidation (left) or carboxylation (right). x = 1, 2, 3 (Modified from Kovalainen et al. 2012)

Stabilization by surface oxidation consists of generation of multiple Si-O bonds which protect from lytic oxidation. The stabilization is carried out at a high temperature either in the exposure of pure oxygen gas (Aggarwal et al. 2013) or in ambient air (Björkqvist et al. 2003, Kovalainen et al. 2012). Pure oxygen gas has been shown to form a stable protection lasting longer than PSi treated with ambient air (Aggarwal et al. 2013). Despite of that, using ambient air seems to be more common for its easy availability (Björkqvist et al. 2003, Kovalainen et al. 2012). Using high temperature is avoidable by performing the reaction at milder temperature for a longer time (Kovalainen et al. 2012) or humidifying the hot air when piped into the reactor (Chen et al. 1996). In fact, some studies have estimated that using a wet oxidation temperature of 400 - 500 °C has an equal oxidation rate than that of the dry oxidation method performed at 800 or 900 °C (Chen et al. 1996). Nevertheless, using dry ambient reaction conditions appears to be a more general procedure since the stabilized sample can be taken immediately to further experiments without using an additional drying equipment.

An unfortunate disadvantage of using oxidation is the instability of the oxidized PSi in the presence of bases. It has been experimentally demonstrated that oxidized PSi is soluble in a potassium hydroxide solution (Björkqvist et al. 2003). Fortunately, hydrocarbonized PSi surface has shown to be a potent alternative stabilization method to improve both oxidation and chemical stability (Björkqvist et al. 2003 Salonen et al. 2004). Contrary to oxidation techniques,

hydrocarbonization requires an additional HF/ethanol-treatment for PSi sample in order to replace the oxide layer on the PSi surface with hydrogen atoms. After that PSi nanoparticles are treated with a continuous flow of nitrogen and acetylene mixture. Heat energy is being employed to activate the covalent replacement of the surface-bound hydrogen atoms with carbon atoms. (Salonen et al 2004) The formed layer is highly hydrophobic showing to be a good carrier of hydrophobic drugs. The hydrophilicity can be increased by annealing the sample above 680 °C. (Salonen et al. 2005) The hydrophilicity is studied by analyzing the humid sorption properties of the cooled sample (Salonen et al. 2004).

Hydrosilylation is another stabilization method. It utilizes some chemicals as an initiator for the stabilization reaction performed in a liquid phase (Buriak et al. 1999, Xia et al. 2005). Some examples of these methods include Lewis base treatment (e.g. ethylene aluminum dichloride) of alkenes and alkenyls (Buriak et al. 1999) or the formation of a more compact polymer network around the surface of PSi (for instance polydimethylsiloxane) (Xia et al. 2005).

2.2.5. Surface modification for *in vivo* applications

Intravenous administration of therapeutic substances has proved to be the simplest strategy for drug delivery. However, a notable disadvantage of using blood circulation as a drug transportation route is that particles are rapidly removed by the *mononuclear phagocyte system* (MPS) (Owens & Peppas, 2006). *Macrophages* are one of the most characterized cell types of MPS which prevent effective drug delivery (Frank & Fries, 1991, Owens & Peppas, 2006). Macrophages indirectly recognize particulates via plasma proteins called *opsonins* which bind to the surface of particulates (Frank & Fries, 1991). The process ends up in the fast clearance of the particulates into liver and spleen as well as to the urinary excretion reducing the bioavailability of a delivered drug (He et al. 2011, Park et al. 2009).

Several studies focus on the chemical modification of PSi surface to prevent the binding of opsonins. Some interesting approaches have already been reported such as covering the surface with proteins (Sarparanta et al. 2012) and carbohydrates (Passirani et al. 1998). In spite of the natural origin of those molecules stabilization with a synthetic but still non-toxic polymer called *poly(ethylene glycol)* (PEG) has awoken high interests among researchers (He et al. 2011, Owens & Peppas, 2006, Park et al. 2009, Rytkönen et al. 2012, Suh et al. 2007). Although PEG has been shown to reduce the opsonization of PSi *in vitro* the problem with short circulation time *in vivo* has not yet been solved. (Rytkönen et al. 2012)

PEGylation is adding PEG chains to a material. PEG can be synthetized as different derivates depending on the type of preliminary chemistry of the PSi surface. Hydrocarbonized particles can be simply PEGylated with hydrophobic forces between the long unsaturated hydrocarbon of oleyl-PEG and the hydrophobic surface of THCPSi (O-PEG) (Fig. 6a). On the other hand, the covalent-conjugation to the hydrocarbon surface has been performed by using O-PEG with an additional methyl group. The methyl is chemically removed for example with acetonitrile in order to enable binding of PEG to the surface. (Rytkönen et al. 2012) The outer tail of the PEG chain provides variety options for functionalization (Owens & Peppas, 2006) although some non-PEG carboxyl and amino linkers have also shown to be effective for covalent conjugations (Mäkilä et al. 2012, Schwartz et al. 2005, Xu et al. 2012). The concentration of PEG and the length of the polymer must be optimized in order to achieve a long-lasting “brush-like” shield (Fig. 6b, c).

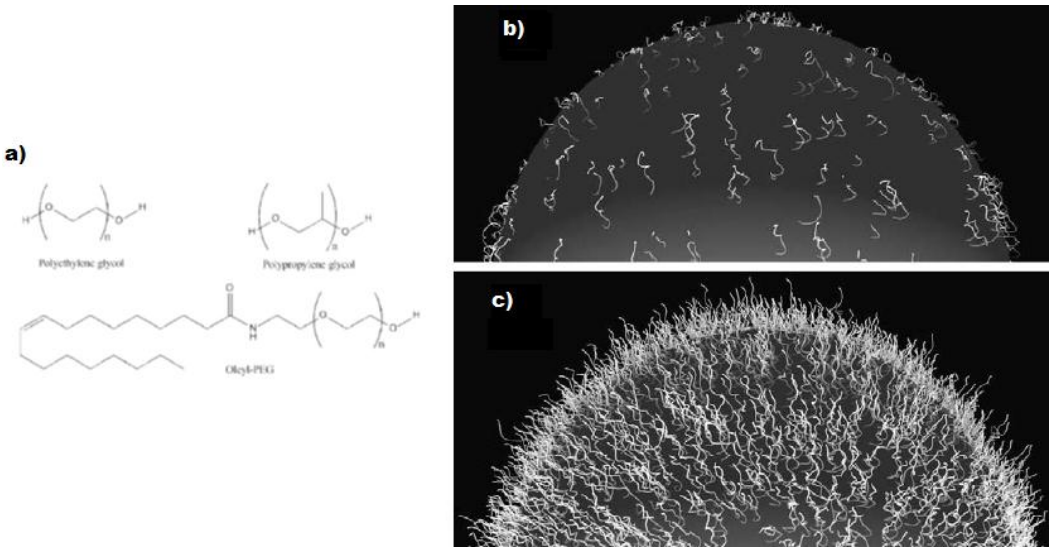

Figure 6. a) The structures of poly(ethylene glycol) (PEG) (left top corner) and its general derivate compounds. The coverage of PEG compounds can be seen in represented three dimensional schematic pictures. **b)** In the low coverage the PEG chains are located near the particle surface. **c)** In the high coverage PEG chains forms a brush-like appearance, which leads to a steric barrier for opsonization (Modified from Owens & Peppas, 2006).

PEGylation changes the structural parameters of the particles. First of all, PEGylation may alter the particle surface charge also known as zeta potential (*ζ*-potential). Furthermore, a PEG layer gives a new size to the particles called *hydrodynamic size*. (Rytkönen et al. 2012) Changes in these two parameters may affect the function of a drug delivery system. For example, Suh et al. (2007) reported that PEGylation of polymeric nanoparticles show clear transportation in HeLa cell line decreasing the portion of the hindered transportation mechanisms by 30 %. Both *ζ*-potential and hydrodynamic size can be measured with a DLS instrument (Rytkönen et al. 2012).

2.3. Porous silicon nanoparticles in targeted drug delivery applications

2.3.1. Strategies to prolong the release of drugs

PSi particles have turned out to be a versatile tool for targeted delivery of small pharmaceuticals. The drugs are loaded inside the pores of PSi particles where they are stabilized against negative effects of various environmental conditions (Salonen et al. 2005, Sarparanta et al. 2012). The simplest loading procedure is based on the hydrophobic interactions between the drug and particle surface. The PSi particles and drugs are simply mixed together in a solvent and incubated for an appropriate time. (Kovalainen et al. 2012, Limnell et al. 2007, Salonen et al. 2005) A pressure caused by ultrasonicating can be used for speeding up the loading (Kovalainen et al. 2012). The loading solvent is chosen according to the solubility of the drug and is in most cases water, ethanol or dimethylsulfoxide solutions (DMSO) (Kovalainen et al. 2012, Limnell et al. 2007, Salonen et al. 2005). The function of the solvent is to drive drug molecules into the pores. The release is tested in a different solvent where the drug diffuses out of the pores. The amount of diffused drug can be determined for example by taking a sample from the supernatant for *high pressure liquid chromatography* (HPLC) measurements. (Salonen et al. 2005)

The solvent is eliminated from the pores by evaporating the solvent from the loaded particles. During the evaporation the drug either crystallizes inside the pores having either a poorly water-soluble perfect crystal lattice or easily-soluble *amorphous* appearance. (Limnell et al. 2007, Salonen et al. 2005, Wang et al. 2010) For example indomethacin exists in both the poorly water-soluble γ-form and more soluble α-form distinguishing with their melting points (Hancock & Parks, 2000).

Although it is complex to control the transition between a crystal and an amorphous form some parameters have already been found. Salonen et al. (2005) showed the phenomenon is dependent on the original solubility of the drug (Fig. 11) while Limnell et al. (2007) reported the

size of the confined space of pores plays also a crucial role. The release experiments of those studies were performed in a buffered salt solution with fixed pH in order to simulate the stability of the delivery system in the different stages of the oral administration route. For targeted drug delivery it is extremely important to always test the release with other simulating mediums, especially in plasma (Tay et al. 2004) in order to get a wider insight of the drug release in the complex intravenous environment.

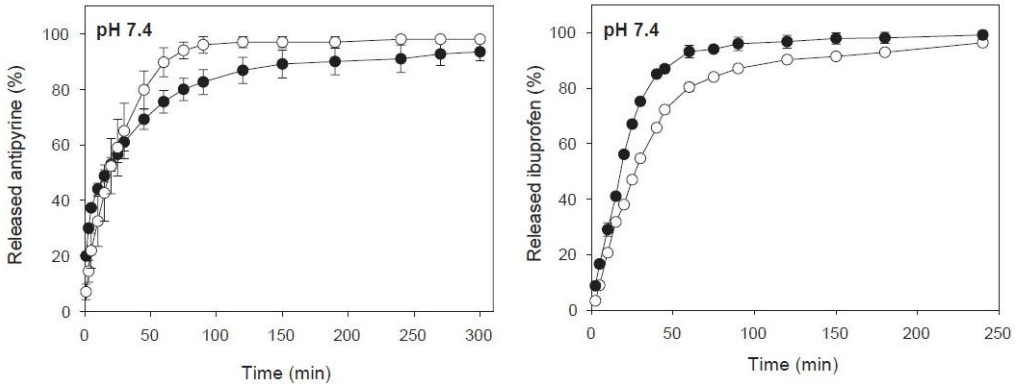

Figure 7. Aqueous dissolution profiles of **a)** loaded soluble antipyrine and **b)** loaded liphophilic ibuprofen from similar size thermally hydrocarbonized porous silicon microparticles with their un-loaded controls (solid and open symbols, respectively) in Hank's balanced salt solution at pH 7.4, +37 °C (n = 3, mean ± sd). (Modified from Salonen et al. 2005)

Reduction of the drug release outside the target tissue, whether it is due to the crystallization process or for *in vivo* factors, is an important goal in the targeted drug delivery applications. Instead of being totally eliminated the release usually follows a zero-order trend (Fig. 8). In targeted delivery, premature drug release has been found to have many negative effects for example uneconomical drug consumption, reduced therapeutic effects in the target as well as toxicity in healthy tissues. Sometimes the initial release is unpredictably rapid occurring within a short time period. The phenomenon is called *burst effect and* its origin is not fully understood. (Huang & Brazel, 2001) (Fig. 8)

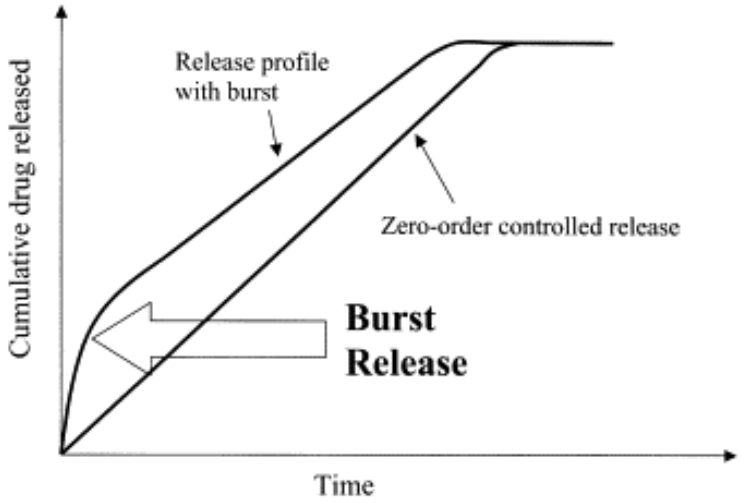

Figure 8. A schematic diagram of the burst effect in a zero - order drug delivery system. (Huang & Brazel, 2001)

Efforts have been done to achieve a controlled release system for targeted drug delivery applications (Huang & Brazel, 2001). Functionalization of the internal surfaces of PSi particles allows drugs to be loaded and trapped by covalently capping the openings of the pores. This technique allows the external surface to stay untouched for other useful modifications. After transportation to a cell the drug release is triggered for instance by enzymatic stimuli (Fig. 9). (Lai et al. 2003) However, it has been noticed that it is challenging to add functional groups selectively into the internal space of the etched particulates (Trewyn et al. 2007).

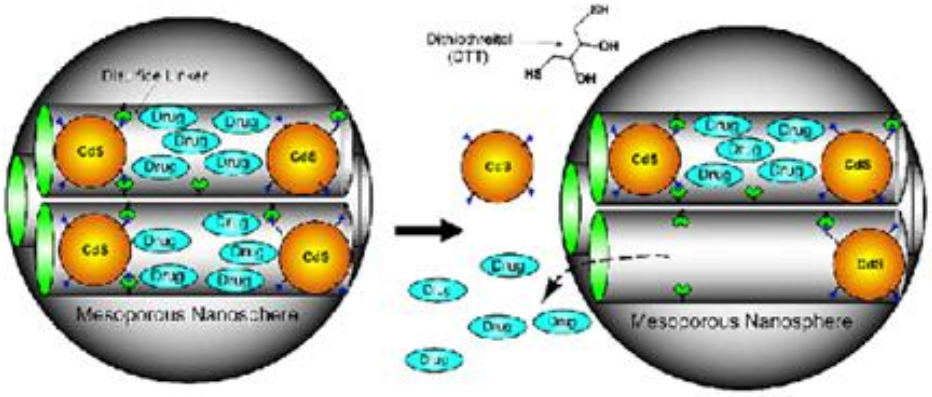

Figure 9. A schematic example of prevent the escape of drugs from the pores by sulfide-functionalized cadmium nanoparticles (CdS) *in vitro.* The cleavage of the disulfide-bridges is trigger by a dithiothreitol (DTT) reducing agent. (Lai et al. 2003)

Another interesting method for coating and crosslinking of polymeric material includes cellular stimuli responsive polyelectrolytes (De Villiers et al. 2011). For example chitosan and dextran sulfate are used (Yuan et al. 2010). The subunits are adsorbed to the surface of particles as positively and negatively charged monolayers, which results a multilayer coating. This method called *layer-by-layer self-assembly* (LBL) and it has been used for inhibiting dissolution of microcrystal drugs (Shenoy et al. 2004, Qiu et al. 2001). Furthermore, some LBL produced nanocoatings have other advantages (De Villiers et al. 2011). For instance, an increase in the antibacterial property of silver nanoparticles has been reported (Yuan et al. 2010).

2.3.2. The concepts and characterization of drug loading and release

Several concepts have been created to express the drug loading results. One is the *specific surface area* (SSA) which consists of the total surface area per unit of the particle mass. The higher the amount of pores the larger is the value of the SSA. A wider SSA increases the likelihood of drugs to interact with the surface of a carrier. On the other hand, the small volume of pores means the fact that only few drugs are capable to fit into the narrow internal space of the small nano-pores. (Limnell et al. 2007)

The amount of the loaded drug is generally expressed as *loading degree* using the dry weight of both the loaded drug and particles (Eq. 1) Un-covalent drug loading prefer to end up a heterogenic equilibrium between the loaded and un-loaded drug (Salonen et al. 2005).

$$\text{Loading degree} = m_{\text{drug loaded}} / (m_{\text{drug loaded}} + m_{\text{particle}}) \times 100\ \%\ \text{w/w} \quad \text{(Eq. 1)}$$

The calculated value of % w/w varies significantly not only for physico-chemical properties but also used analytic method. For instance, Salonen et al. (2005) reported the computational N_2 sorption technique to yield erroneous results due to the blockage of pores by drugs. In order to increase the reliability of measured results of quantity and the state (2.4.1.) of a drug inside the pores, different characterization methods such as XRD and HPLC should be used simultaneously (Kovalainen et al. 2012, Limnell et al. 2007, Salonen et al. 2005, Wang et al. 2010)

2.3.3. Model drugs

In drug delivery studies, model drugs are used to give insight in which particle type is the most suitable one for drug carrier functions. A compound is accepted for drug delivery studies if it shows *drug-likeness.* Drug-likeness is determined according to *Lipinski's rule of five* (RO5) named by its developer in 1997 (Lipinski et al. 1997). Originally, the conditions of RO5 were settled down for improving screening of *orally bioavailable* substances from the abundance of compounds with varied physicochemical properties cumulated from numerous combinatorial and medicinal studies. RO5 is based on the observation that oral bioavailability, the condition for the achievement of the phase II clinical status, is associated with molecular size (molecular weight ≤ 500), the partition efficient logP (log ($c_{octanol}$ / c_{water}) ≤ 5) and also the number of hydrogen bond donors and acceptors (≤ 5 and ≤ 10, respectively). (Lipinski, 2004, Lipinski et al. 1997)

During the last decade drugs with different pharmacological functions are widely used as a model drug for PSi drug delivery studies (Limnell et al. 2007, Salonen et al. 2005, Vallet-Regi et al. 2001, Wang et al. 2010) (Fig. 10. compounds 1 - 6). D-LH_2 passes also all of the RO5 conditions (Fig. 10. compound 7). The major biological function of D-LH_2 is to serve as a substrate for the bioluminescence reaction catalyzed by FLuc (White et al. 1969) although some recent studies have shown it to have pharmacologically interesting functions (Hu et al. 2012).

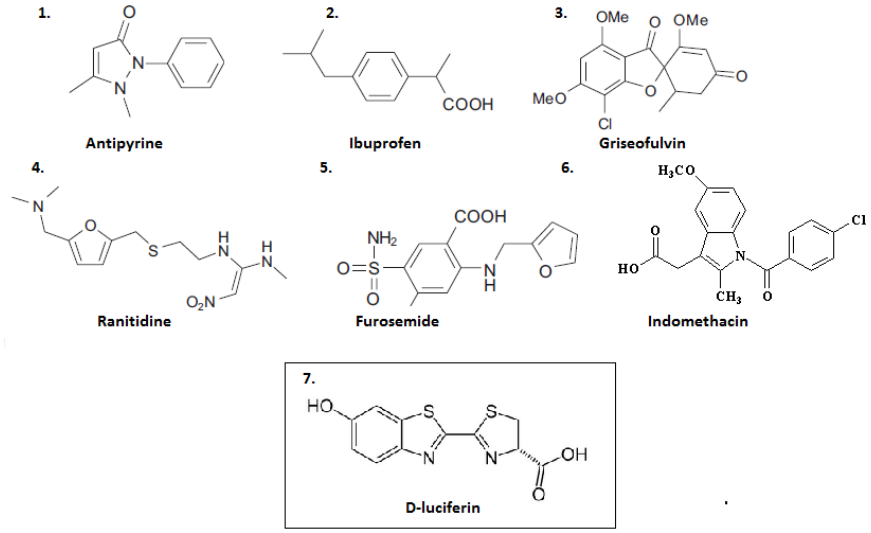

Figure 10. The structures of model drugs (1 - 6) and other drug-like compounds (7) found in research publications. (Modified from Salonen et al. 2005)

2.3.4. Labels for drug delivery studies

The properties of a drug delivery system can be studied by labeling the particles. Furthermore, some labeling methods enable to study the loading and release of a cargo if label-free methods cannot be utilized. For instance, labelling may be preferred if a drug have too weak fluorescence properties for spectroscopic measurements.

There are several different labels for nanoparticle research. Radioactive labels, such as iodine 125 isotope, are used for systemic biodistribution (Rytkönen et al. 2012) and cellular internalization studies (Bimbo et al. 2010). Radioactive labels are remarkable useful for labeling aromatic cargos without changes in the structure-related properties (Rytkönen et al. 2012). For instance, iodine 125 has been added into the structure of indomethacin (El-Ghany et al. 2005) and tyrosine (Rytkönen et al. 2012) with a simple substitution mechanism of a single atom. Iodine 125 requires oxidation of $^{125}I^-$ to $^{125}I^+$, which can be done for example with IODO-GEN (1,3,4,6-tetrachloro-

3α,6α-diphenyl glycoluril) (Rytkönen et al. 2012) or chloramine T (tosylchloramide sodium) (El-Ghany et al. 2005).

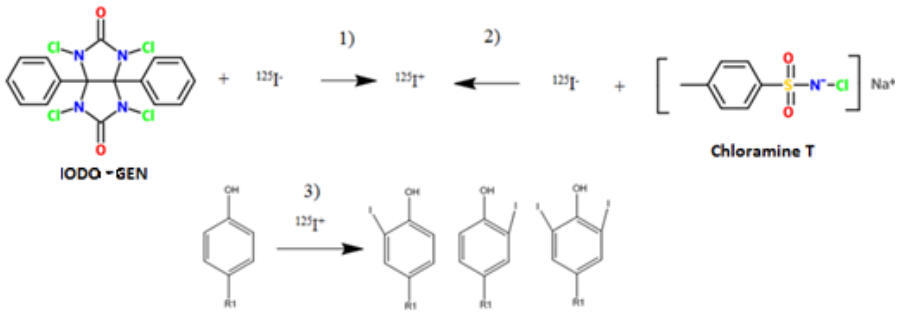

Figure 11. IODO-GEN and chloramine T can be used for labeling of aromatic structures with radioactive iodine 125 isotope. At first, iodine 125 can be oxidized either by **(1)** IODO-GEN or **(2)** chloramine T. **(3)** Then the oxidized iodine is added into a benzene ring. The result depends on the other atoms bound in the structure. In this example R_1 is the determinant. (Modified from Pubchem Compound, 2014)

On the other hand, the high energy of the radiation causes a safety risk which must be taken account by a researcher (Gjøen & Berg, 2001). Moreover, the radiation of a radioactive label cannot give detailed information about the intracellular location of the label. This means, one cannot truly tell whether the labeled object is in the nucleus, the cytoplasm or trapped by endosomal system leading to degradation (Varkouhi et al. 2011).

For intracellular imaging of nanoparticles fluorescent labels are widely used. One example is a fluorescent compound called fluorescein isothiocyanate (Bimbo et al. 2010) (PubChem ID 18730). Fluorescent labels are more used for labeling particles than pharmaceuticals because they are likely to change the structure-related properties of a drug. The cellular localization of the labelled particles is studied by confocal microscopy (Piepenhagen et al. 2010) but the label must be excited by an external source of radiation before it is capable of emitting light. Unfortunately, cells are susceptible to *phototoxicity.* In phototoxicity multiple excitations of a fluorescent label generates

singlet oxygen and other reactive oxygen species (Hoebe et al. 2008). The products cause cellular stress having many consequences, for example apoptosis.

3. Experimental section

3.1. The purpose of the study

Mesoporous silicon nanoparticles have been proved to be an effective material for drug delivery applications. The aim of this Master's thesis was to study drug loading and release properties of different mesoporous silicon nanoparticles using D-luciferin as a drug like model molecule. Three types of porous silicon nanoparticles were used (UnTHCPSi, TCPSi-NH_2 and WOPSi-NH_2). The study begins with a preliminary screening of porous silicon nanoparticles continuing to the optimization of the particle concentration and ending up to a simple bioluminescence *in vitro* release study. In the release study D-luciferin serves as a substrate in the light producing bioluminescence reaction catalyzed by luciferase. Loading capacity was determined with fluorescence measurements while the release kinetics was determined using a luciferase-rich release buffer and a luminometer instrument.

3.2. Materials and methods

3.2.1. General information of the nanoparticles

In the current study three amino or carboxyl terminated PSi nanoparticles (UnTHCPSi, TCPSi-NH_2 and WOPSi-NH_2) were used. The surface groups allows covalent functionalization for instance with peptides (Mäkilä et al. 2012). All the particles had an average particle size between 170 and 180 nm while pore diameter was around 10 nm. The batches were stored in 99.5 % ethanol (ACS

Reagent, Thermo Fischer Scientific, Helsinki, Finland) at -20 °C and were sonicated for couple of seconds before use (Branson Ultrasonicator, Danbury, USA).

3.2.2. TCPSi-NH2 and WOPSi-NH2 particles (amino particles)

In this study two types of amino modified porous silicon nanoparticles were used. TCPSi-NH_2-particles are thermally carbonized nanoparticles covered with primary amino groups (Fig. 12). WOPSi-NH_2-particles are wet-oxidized porous silicon amino nanoparticles which differ from the latter with the oxidized surface. Both amino particles were manufactured with a silane coupling method. The stepwise fabrication procedure includes oxidation of the carbonized/oxidized surface with ammonium hydroxide and hydrochloric acid and further treatment with 3-(2-aminoethylamino) propyldimethoxymethylsilane (AEAPMS) (Xu et al. 2012). Both batches were received from the Department of Applied Physics in the University of Eastern Finland (Ph.D. Wujun Xu). The age of the TCPSi-NH_2 batch was 5 months while the WOPSi-NH_2 particles were one year old. The zeta potential (ζ-potential) of the particles was +60 mV (Xu et al. 2012).

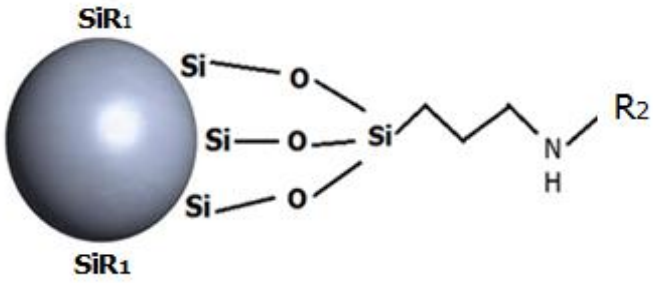

Figure 12. The surface structure of TCPSi-NH_2 and WOPSi-NH_2 particles (R_1 = C_x and $CH_2CH_2NH_2$).

3.2.3. UnTHCPSi particles (carboxylated particles)

UnTHCPSi particles were used in order to have a point of contrary to the amino particles. UnTHCPSi particles are thermally hydrocarbonized porous silicon nanoparticles with covalently attached 1-undecylenic acid chains on outer surface (Fig. 13). The UnTHCPSi-particles were manufactured by doctoral student Martti Kaasalainen in the Department of Physics and Astronomy in the University of Turku. (Kaasalainen et al. 2012, Kovalainen et al. 2012) The same particle batch was used in other studies (Rytkönen et al. 2012). The ζ-potential was around -40 mV.

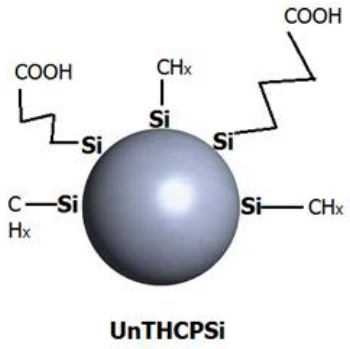

Figure 13. The surface structure of UnTHCPSi particles.

3.2.4. Luciferin and luciferase

QuantiLum® recombinant firefly luciferase (FLuc) was purchased from Promega (USA) and prepared for 100 µg/ml aliquots. The storage buffer was prepared by following the manufacturer's instructions and contained 25 mM Tris-Acetate (pH 7.4) (Sigma - Aldrich, St Louis, USA), 1 mM EDTA (Sigma - Aldrich), 1mM DTT (YA Kemia, Helsinki, Finland), 0.2 M ammonium sulfate (Riedel-de Haen, Seelze, Germany), 15 v/v % glycerol (BDH Prolabo, Helsinki, Finland) and 30 % v/v ethylene glycol (Merck Worldwide, Espoo, Finland). Before the use the aliquots were

stored at -74 °C and melted at room temperature. A careful mixing of the aliquot with a pipette was required to remove the enzyme from the bottom of the tube. Poorly water soluble D-LH_2 free acid (Sigma Aldrich; purity ≥ 99 %) was diluted to 2 mg/ml 99.5 % ethanol stock (ACS Reagent, Thermo Fischer Scientific, Helsinki, Finland) and stored at +4 °C in the darkness to avoid racemization (Nakamura et al. 2005, Seliger et al. 1961).

3.2.5. Release buffer

A buffer solution for D-LH_2 enzymatic release studies with FLuc was prepared according to manufacturer's instructions with small modifications before the release experiment (Sigma - Aldrich, 2011). The prepared release buffer contained 4.4 mM magnesium sulfate heptahydrate (Sigma - Aldrich, Germany) and 1mM ATP (100 mM aqueous stock stored at -20 °C and melted at need) (Sigma - Aldrich, Germany) 1 x phosphate buffer saline (PBS) (Sigma-Aldrich, Germany) at pH 7.4. For preventing the aggregation between the nanoparticles bovine serum albumin fraction V (BSA) (VWR Prolabo, Celdenaaksebaan, France) was used achieving 0.01 w/v % concentration in the release buffer.

3.2.6. Spectrometer and other instruments

The washing of particles as well as loading and release tests were performed using sonication and centrifugation steps which were carried out with a Branson 2510E-MT Ultrasonicator instrument (Branson, Danbury, USA) and Eppendorf centrifuge 5415D (Eppendorf AG, Hamburg, Germany). Centrifugations were performed with a standard speed of 13,200 rounds per minutes always at room temperature. The samples were pipetted to a Lumitrac 200 96 fluorescent plate (Greiner-Bio-One GmbH, Frickenhausen, Germany) for measuring the light emission. The fluorescent and luminescent measurements were performed with Fluoreskan/Luminoskan spectrophotometer (Thermo Fischer, Helsinki, Finland) at room temperature using Ascent Software Version 2.6.

3.2.7. The standard line of D-luciferin fluorescence

The fluorescent of D-LH_2 was measured with different concentrations of D-LH_2 in order to find the linear concentration range of D-LH_2. The standard line gave evidence which amount of D-luciferin should be used for the loading studies.

The D-LH_2 stock (2 mg/ml) (Sigma - Aldrich, USA) was diluted to 400 µg/ml of water. The stock solution, a 96-well plate, deionized water and a multichannel pipette was used for preparing the final 1 : 4 dilution series including concentrations from 0 to 250 µg/ml. Fluorescence was measured at room temperature. The excitation wavelength was 320 nm whilst the emission wavelength was kept as 538 nm.

3.2.8. Comparison loading properties of mesoporous silicon particles

In this study three types of particles (UnTHCPSi, TCPSi-NH_2, WOPSi-NH_2) were used in order to study the effect of the surface chemistry on the loading of D-LH_2. The dilutions of D-LH_2 were prepared by following the previously prepared D-LH_2 fluorescence standard line.

Before starting the study 50 µg of nanoparticles were washed and resuspensed to 2 mg/ml concentration using deionized water. The D-LH_2 stock (2 mg/ml in water) was diluted to a concentration 200 µg/ml for the loading experiment. One 25 µl sample of the D-LH_2 dilution was mixed with 25 µl of the nanoparticle suspension. The control sample was prepared identically replacing the particle suspension with deionized water.

The loading was performed by incubating the samples at room temperature for one hour sonicating every 13 minute for 2 minutes. The procedure was finished with centrifugation for 10 minutes. 25 µl of the supernatant was transferred to a 96-well plate for the fluorescence measurement. The loading degree and loading efficiency ($m_{drug\ loaded}$ / ($m_{drug\ loaded}$ + $m_{un\text{-}loaded}$) × 100 %) were determined.

3.2.9. Optimization the particle concentration for loading studies

The TCPSi-NH_2 particles were chosen for further studies because they showed the highest values of loading efficiency and loading degree. For this experiment a standard concentration of D-LH_2 was loaded to the nanoparticles with variable particle concentrations. The method enables to find the concentration for both the cargo and the nanoparticles which can be used for reaching a sufficient loading efficiency to simplify performing a release experiment. In this study 90 % loading efficiency was estimated to be sufficient for using the loading suspension directly for the release studies without an interfering background signal.

At first, TCPSi-NH_2 particles (680 µg) were washed three times and suspended to 3.6 mg/ml using deionized water. 17.5 µl of the D-LH_2 stock (2 mg/ml) was diluted to 140 µg/ml of deionized water. The particle suspension was divided into five separate batches. D-LH_2 and deionized water and particles were added in order to obtain 100 µl samples with 70 µg/ml of D-LH_2 and one 400, 800, 1400, 1600 or 1800 µg/ml of particles. The control sample was prepared identically but without nanoparticles. After that the loading was performed like previously. 20 µl of each sample was transferred to three parallel wells on a 96-well plate with 80 µl of water (1 : 5 dilution). The fluorescent was measured and the loading degree and loading efficiency were calculated for each sample as previously mentioned.

3.2.10. Optimization the particle concentration for release studies

Porous silicon nanoparticles are well-known to absorb light emitted from an external light source. The effect is likely to cause a loss of light signal in the very end of the kinetics measurements of luminescence reaction between FLuc and D-LH_2. For this reason the nanoparticles were diluted with a constant concentration of D-LH_2 in order to reduce light absorption caused by the particles. One of the particle concentrations was chosen by finding an intersection point in the dilution

series where the total light emission from the D-LH_2-particle mixture is equal to the one of the control sample without any particles.

At first, 213 µg of TCPSi-NH_2 particles were washed three times with deionized water. The particles were diluted to 323 µl of the release buffer and mixed with 10 µl of D-LH_2 (0.9 mg/ml in water). The prepared suspension was quickly sonicated and 100 µl samples were transferred immediately to three wells on the multiwell plate. The control sample was processed with the same method but without particles.

Using a single-channel pipette and the release buffer the 1 : 2 dilution series for both new-loaded particle suspension and the control sample was prepared (50 µl/well). The reaction was initiated by adding 50 µl of the recombinant FLuc (20 µg/ml in the release buffer) to each well. Thus, each well contained a nanoparticle concentration of 0, 10, 20, 40, 80, 160 or 320 µg/ml and a D-LH_2 concentration of 0.4, 0.8, 1.6, 3, 7 or 14 µg/ml. Furthermore, each well contained a constant 10 µg/ml concentration of FLuc. The luminescence was measured using the spectrophotometer.

3.2.11. Study the drug release properties of mesoporous silicon nanoparticles using the bioluminescence of D-luciferin

Based on the above-mentioned results of the loading studies the final study about release kinetics of the nanoparticles was performed. The release kinetics was studied with luminescent reaction initiated by the recombinant FLuc mixture.

At first, 100 µg of TCPSi-NH2 nanoparticles were washed three times and resuspended to 3.2 mg/ml using deionized water. The suspension was divided to two separated 25 µl samples serving as a loading sample and non-loading sample. 25 µl of D-LH_2 (140 µg/ml in water) was added to the first sample and loading was performed like previously described.

For kinetics measurements, samples were transferred to three wells of a 96-well plate (Fig. 14). Six other wells were reserved for parallel samples (n = 3). To the first well, 5 µl of the loaded particles (8 µg) was transferred. To the second well, 2.5 µl of D-LH_2 (350 ng) was added with 2.5 µl of the un-loaded particles (8 µg). The loading of D-LH_2 into the particles was prevented by keeping those drops apart on the opposite sides of the well until adding the FLuc recombinant mixture. To the last well, 2.5 µl of D-LH_2 (350 ng) was added as a single drop with 2.5 µl of deionized water (control 2). This gives more data for comparison the results of loaded and un-loaded particles. The plate was placed inside the luminometer. The lid of the instrument was opened for injecting 95 µl of the FLuc recombinant (950 ng) in the release buffer to each well. The volume of the release buffer was fixed for simulating the injection of the particles to a mouse. The luminescence was measured with one minute intervals. The measurement was continued at room temperature in the darkness for 18 hours.

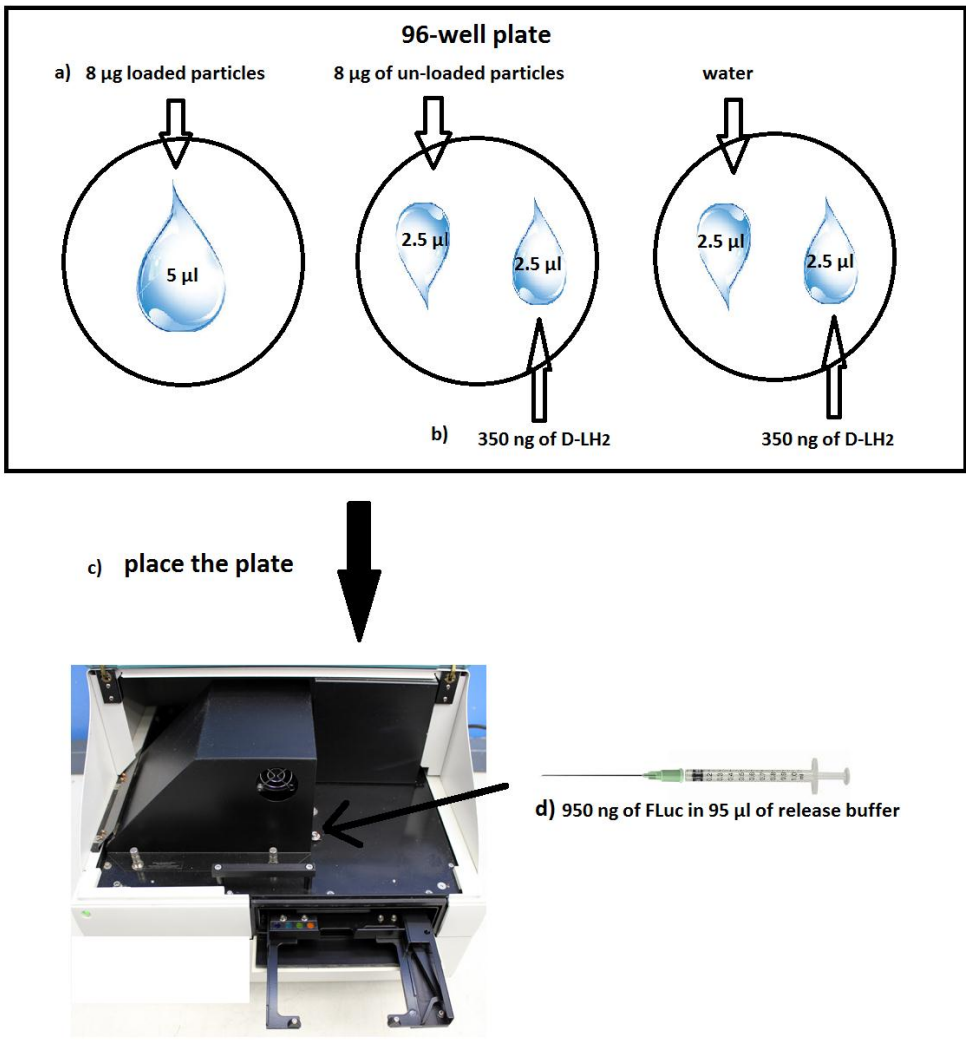

Figure 14. A novel method for studying the release of D-luciferin (D-LH_2) using mesoporous silicon nanoparticles. The samples were prepared using three wells of a 96-well plate. **(a)** At first D-LH_2 loaded and un-loaded particles as well as water were added. **(b)** Drops of D-LH_2 were added to the opposite site of un-loaded particles and the water drop. **(c)** The plate was transferred into the luminometer. **(d)** The lid was kept opened and a surplus of FLuc was injected to each well for starting the reaction. The lid was closed immediately and the light was measured with a luminometer in the darkness over the time.

3.3. Results

3.3.1. The standard line of D-luciferin fluorescence

According to the results, the linear concentration range of D-LH_2 for the used spectrophotometer is 0 - 110 µg/ml.

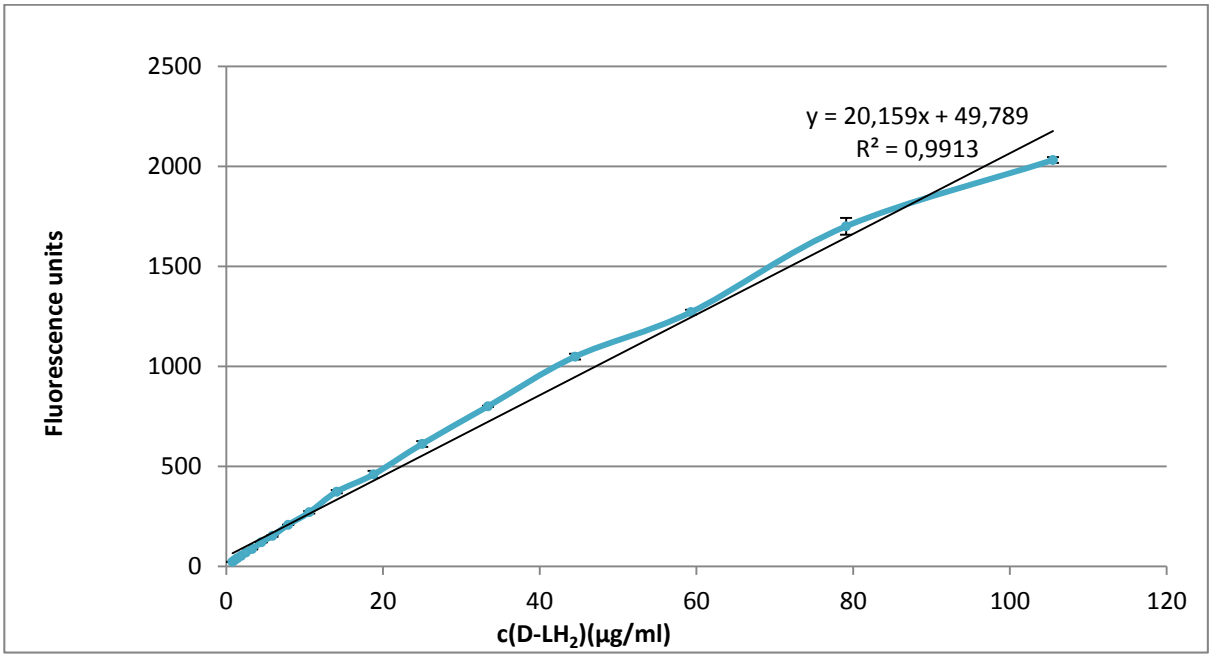

Figure 15. The linear relation of aqueous D-luciferin (D-LH_2) concentration to the fluorescence at room temperature using Fluoroskan/Luminoskan spectrophotometer instrument (Thermo Fischer, Helsinki, Finland) with an excitation wavelength of 320 nm and an emission wavelength of 538 nm. The error bars indicate standard deviations. (n = 3)

3.3.2. Comparison the loading properties of different porous silicon particles

D-LH_2 had the highest loading efficiency to the TCPSi-NH_2 nanoparticles (68 %) (Fig. 16). TCPSi-NH_2 also reached to the best loading degree (12 % w/w) over the tested particles (UnTHCPSi 1 % w/w and WOPSi-NH_2 4 % w/w). According to these results, TCPSi-NH_2 is the most potent carrier for D-LH_2.

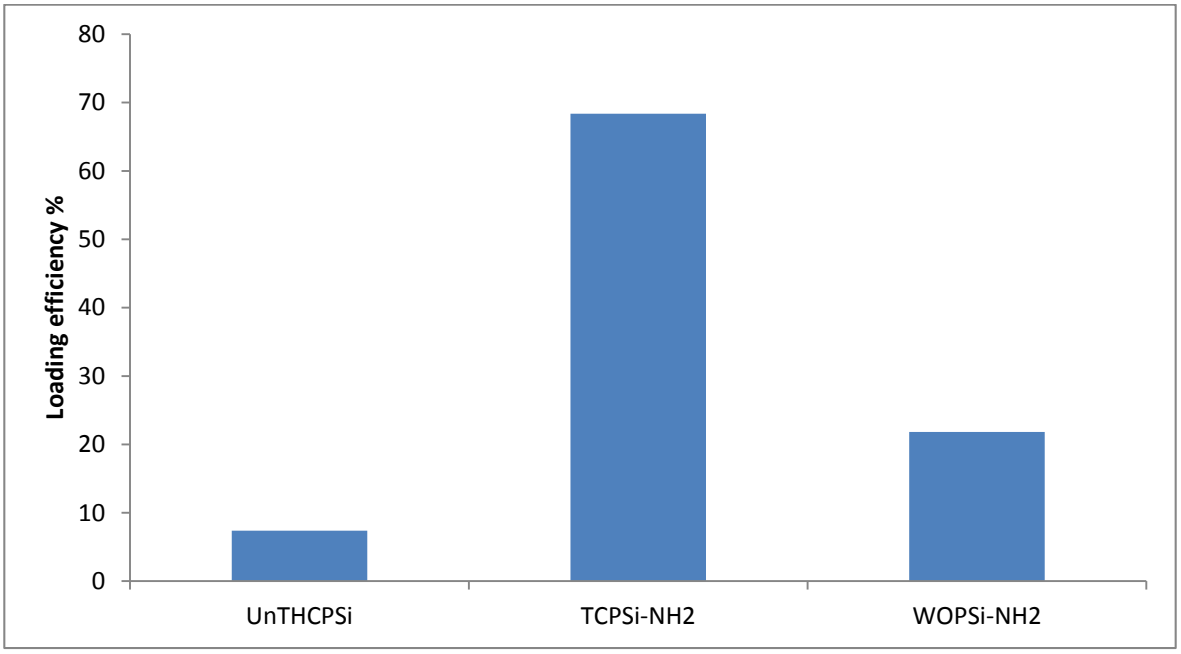

Figure 16. The loading efficiency of D-luciferin into three types of porous silicon nanoparticles in water after 1 hour incubation at room temperature (n = 1). The samples were sonicated every 13 minutes for 2 minutes. The loading was carried out with 10 µg of D-luciferin and 50 µg of the nanoparticles in 50 µl of deionized water. The control sample contained 10 µg of D-luciferin in 50 µl of deionized water without nanoparticles expressing 100 %.

3.3.3. Optimization the particle concentration for loading studies

The comparative loading study showed the TCPSi-NH_2 particles to be the best alternative for the optimization steps. The aim of the optimization is to find the amount of TCPSi-NH_2 particles which shows over 90 % loading efficiency for D-LH_2 loading. 90 % loading efficiency was estimated to be sufficient for using the loading suspension directly for the release studies without an interfering background signal. In this study 93.9 % loading efficiency was achieved by using 140 µg of TCPSi-NH_2 nanoparticles, 7 µg of D-LH_2 in 100 µl of water (the fourth data point in the figure 19). This means that 6.6 µg of D-LH_2 was loaded. With 140 µg of TCPSi-NH_2 a loading degree of 4.48 % w/w was achieved (table 1).

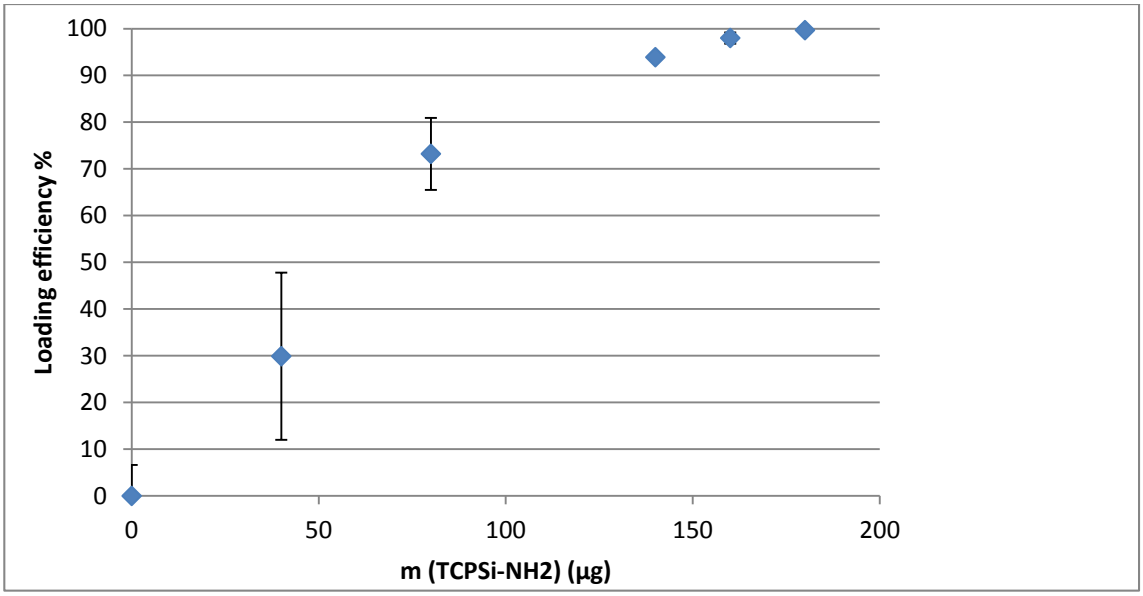

Figure 19. Unbound D-luciferin in the loading supernatant after loading with five different concentrations of TCPSi-NH_2. The loading was performed with 7 µg of D-luciferin in 100 µl of deionized water. The loading was carried out by incubating at room temperature for one hour. The control sample was 7 µg of D-luciferin in 100 µl of deionized water expressing 100 %. The error bars indicate standard deviations. (n = 3)

Table 1. Average loading degrees using 7 µg of D-luciferin with different concentrations of TCPSi-NH_2 nanoparticles in 100 µl of water.

m (TCPSi-NH2) (µg)	40	80	140	160	180
% w/w	4,97	6,02	4,48	4,11	3,73

3.3.4. Optimization of the particle concentration for release studies

The D-LH_2 loaded TCPSi-NH_2 particles were diluted for the luminescence measurement in order to minimize the light absorption by TCPSi-NH_2 during the enzymatic release studies. According to the results 2 µg of TCPSi-NH_2 nanoparticles does not cause significant light absorption of 86 ng of D-LH_2 in 100 µl of water. (Fig. 20) This means that the loading sample should be diluted to a concentration 20 µg/ml for measuring the luminescence.

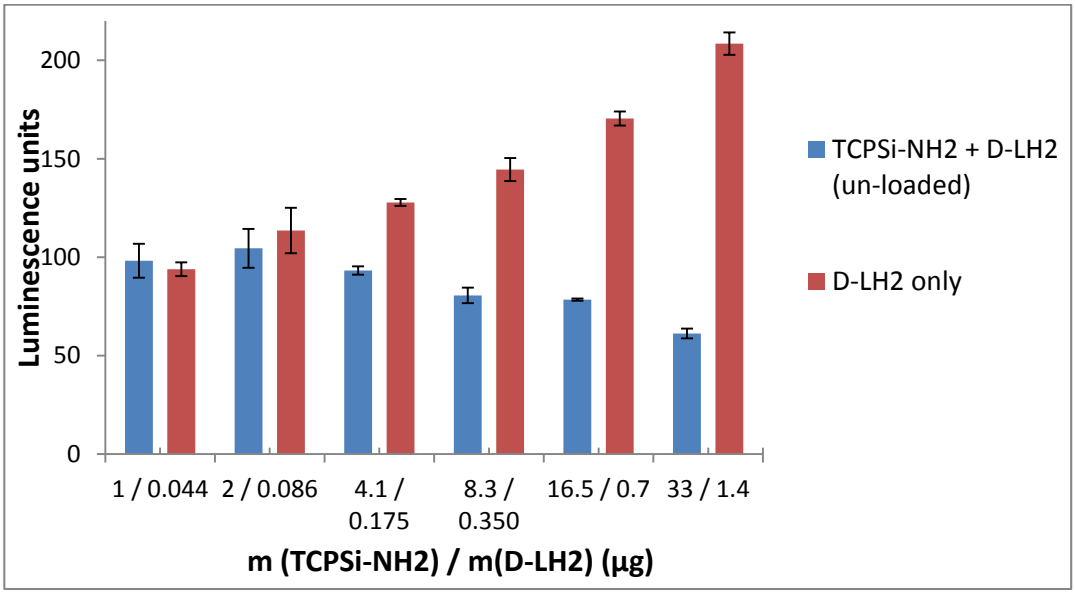

Figure 20. Luminescence for un-loaded TCPSi-NH_2 nanoparticles with D-luciferin and a particle free D-luciferin solution in 100 µl of deionized water. The reaction was started with 950 µg of Luciferase. The error bars indicate standard deviations. (n = 3)

3.3.5. Study the drug release properties of mesoporous silicon nanoparticles using D-luciferin

The experimental parameters for the release study with the bioluminescent reaction between D-LH_2 and Fluc were chosen according to the following observations made above

1. The linear concentration range of D-LH_2 for the used fluorescence/luminescence instrument is 0 - 110 µg/ml.
2. Among the three tested nanoparticles TCPSi-NH_2 is the most suitable as carrier for D-LH_2.
3. 140 µg of TCPSi-NH_2 nanoparticles are sufficient for achieving over 90 % loading efficiency when loaded with 7 µg of D-LH_2 in 100 µl of water. With these amounts a loading degree of 4.5 % w/w is reached.
4. The D-LH_2 loaded TCPSi-NH2 nanoparticles need to be diluted to a concentration 20 µg/ml for the enzymatic release study.

For the release study the loading procedure was repeated. The average loading efficiency of D-LH_2 into TCPSi-NH_2 was 76 % and the calculated loading degree was around 3.2 % w/w. The values differ from the previous loading results (Fig. 19; Table 1). The difference between the loading results may be explained with the differences between the sonication conditions which are explained with the fact that particles were sonicated by keeping the samples by hands on the water bath of the sonicator.

In the current study the particle concentration was adjusted to a concentration 80 µg/ml in order to verify the results of the previous optimization study (3.4.5). Indeed, the kinetic data curve (Fig. 21) shows a higher luminescence level for the sample without particles suggesting light absorption by the particles.

There are no significant differences between the luminescence values of the loaded nanoparticles and the non-loaded particles over the time reflecting the fact that almost all the D-LH_2 is rapidly released out of the particles. The major difference between loaded and un-loaded nanoparticles is noticed within the first minute. In the beginning the luminescence stayed 1.8 times weaker with loaded nanoparticles than the one of the non-loaded D-LH_2-TCPSi-NH_2 mixture. Still, the initial burst effect of D-LH_2 release is remarkable. After 10 minutes from the initiation the levels of luminescence of the both are equal till end of the measurements.

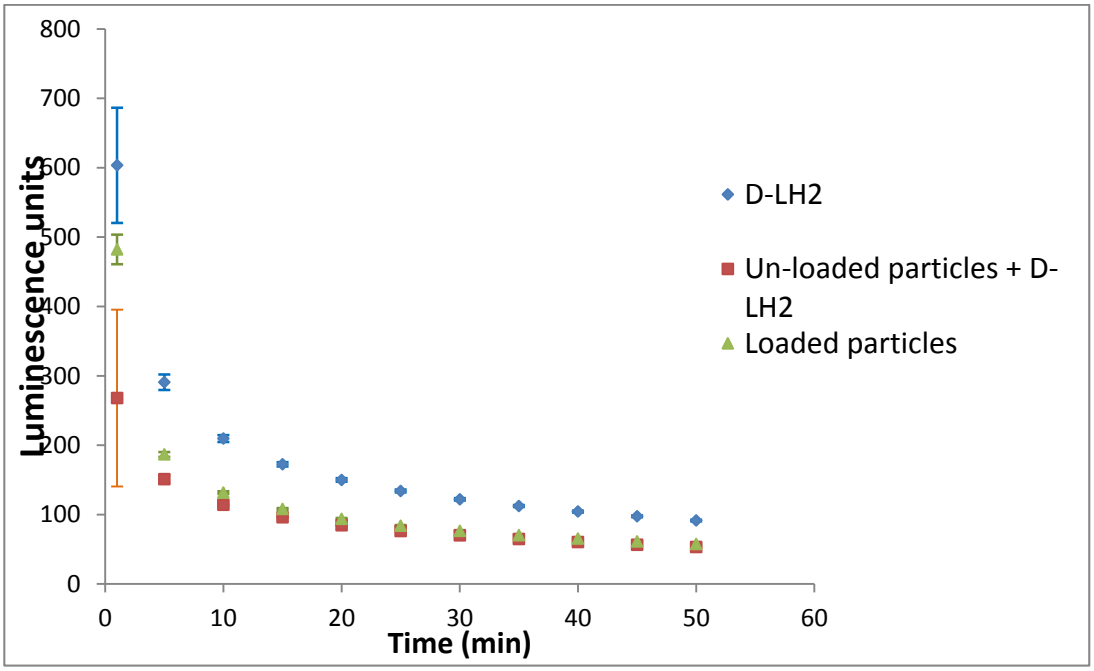

Figure 21. A diagram of the luminecence either TCPSi-NH_2 nanoparticles loaded by D-luciferin, non-loaded TCPSi-NH2 nanoparticles mixed with D-luciferin and free D-luciferin. For the measurement 5 µl of the loading suspension was used containing 350 ng of D-luciferin and 8 µg of TCPSi-NH_2 nanoparticles. The first control contained 8 µg of TCPSi-NH_2 nanoparticles with 350 ng of D-luciferin of un-loaded D-luciferin in 5 µl of water. The second control contained 350 ng of D-luciferin in 5 µl of water. The reaction was started by adding 950 ng of luciferase in 95 µl of the release buffer. Here the used loading efficiency is 100 % for clarity (the achieved loading efficiency was 76 %). Time-scale has also been reduced. The error bars indicate standard deviations. (n = 3)

3.4. Discussion

3.4.1. Loading

In the first part of the current study the loading of D-luciferin (D-LH_2) into mesoporous silicon nanoparticles was studied. The studied particles were coded according to their surface chemistries as undecylenated thermal hydrocarbonized, amino carbonized and amino wet-oxidized porous silicon nanoparticles (UnTHCPSi, TCPSi-NH_2, WOPSi-NH_2, respectively). The loading capacity of the particles was compared in order to find the best candidate for the following optimization step.

The effect of the surface chemistry and pH. Like already stated, D-LH_2 is well-known as poorly soluble drug-like compound. Both the TCPSi-NH_2 and UnTHCPSi have hydrophobic carbonized and hydrocarbonized surfaces, respectively, so it is expected that the D-LH_2 would have a strong interaction to both of the particles. UnTHCPSi loading was predicted to be more efficient because it is more hydrophobic than TCPSi-NH_2. Surprisingly, the results of this study indicated that TCPSi-NH_2 had a higher loading efficiency (68 %) than UnTHCPSi (7 %) and also a better loading degree (12 % w/w, 1 % w/w, respectively). The difference in the loading capacities is explained with the pH of the loading solvent. In neutral water D-LH_2 is mostly in the deprotonated form due to the small value of pK_a (2.93) indicating a strong electrostatic attraction between the negatively charged thiazoline-carboxylic acid moiety of D-LH_2 (Fig. 1.) and the positively charged TCPSi-NH_2-particles.

Decreasing the pH would make D-LH_2 far more acidic and also more hydrophobic, which increases the relevance of the hydrophobic forces to the loading like it was demonstrated with ibuprofen (Limnell et al. 2007, Salonen et al. 2005). More acidic environment would also decrease the charge of UnTHCPSi particles weakening the surrounding barrier enhancing the D-LH_2 loading. However, avoiding pH manipulation is preferred due to the risk of aggregations within particles, which may

interfere the loading. In spite of the risk of particle aggregation, it would be interesting to study the effect of pH with freshly manufactured nanoparticles including also particles without surface modifications. Furthermore, the age of the used particle batches may have had an influence to the loading. To be precise, the UnTHCPSi batch was several months older than TCPSi-NH_2 and may have been oxidized during the storage and the use in the previous studies.

The low loading capacity of the WOPSi-NH_2 contrary to the TCPSi-NH_2 particles cannot be explained with the ζ-potential values. Instead of the surface groups the explanation can be found in different surface stabilization chemistries. The long storing time before the start of the experiment is also to have disturbed to the structure of WOPSi-NH_2 particles having an influence in the loading results. The current loading experiment should be repeated using similarly aged particles while increasing the amount of parallel samples from one to three.

The location of the loaded D-LH_2. The current report does not show the exact location of the loaded D-LH_2 on the particle surface. D-LH_2 may be either accumulated to the pores or be partly adsorbed to the external surface. For sustained release it is more preferred to get D-LH_2 to be loaded into the pores of PSi from which the escape is difficult. For an extended analysis of the success of loading some other analysis techniques are required. For instance N_2 ad/desorption analysis and X-ray diffraction measurements are often run for many model drugs to study the portion and the physical state of a drug in porous silicon pores (Limnell et al. 2007, Salonen et al. 2005, Wang et al. 2010). Nonetheless, the introduction of these methods to a study should be evaluated before the use because the most of them includes additional steps for sample preparation like solvent evaporation. Evaporation may form crystal and amorphous forms of D-LH_2 like it has observed to be happened with small pharmaceuticals (Salonen et al. 2005). Changes in a solid-state of D-LH_2 during the evaporation may have unpredictable impacts on the release as well as on the bioluminescence activity.

Effect of loading solution. Drug loading is also affected by the composition of the loading solution. Changing the solution may improve loading. Poorly soluble drugs which usually are not loaded

using water because it is hard to achieve sufficient drug concentrations. Since D-LH_2 is a poorly water soluble molecule an optional loading solution might be a water-ethanol mixture.

3.4.2. Release

Another aim of this Master's Thesis was to study the D-LH_2 release from porous silicon nanoparticles. The release study was enzymatically performed with recombinant firefly luciferase (FLuc). D-LH_2 is capable to be detected by measuring the visible light produced in the bioluminescence reaction catalyzed by FLuc. TCPSi-NH_2 was chosen because of the best D-LH_2 loading previous loading results among the studied particles.

The D-LH_2 release kinetics. The original hypothesis was that the release of D-LH_2 from TCPSi-NH_2 particles is sustained, which reduces the initial burst effect while prolonging the luminescence time. However, this study failed to achieve a constant release of D-LH_2 which was demonstrated by comparing the light emission of non-loaded and loaded TCPSi-NH_2 samples (Fig. 21). The high initial peak in the luminescence spectrum shows a rapid release of out of the particles. If the burst really occurs it may be a consequence of un-preferred loading to the external surface of the particles. It is reasonable to repeat the experiment by washing the loaded particles couple of times for external bound D-LH_2. If the burst still occur in spite of washing, other techniques to achieve a controlled drug release should be tested. For example layer-by-layer self-assembly is worth applying (De Villiers et al. 2011, Yuan et al. 2010).

The effect of the release medium. The suitability of the release medium should also be reconsidered. In this study the medium included 0.01 % w/v of bovin serum albumin (BSA). BSA was observed decreasing the aggregation between the particles during the release (data not shown) but the release medium requires optimization for D-LH_2. The release medium would be exchanged another such as plasma in order to get better insight of the D-LH_2 release after administrating to the body system.

The effect of the pore size. It is not known if the pore size was incorrect for sustained D-LH_2 release. Furthermore, too high pore size may allow the diffusion of luciferase into the particles. In that case the current release study shows the light which is produced inside the particles. This means there should not be significant restrictions for light coming outside from the pores. For example particles can absorb light in spite of whether the light comes from outside or inside the particles. The effect of the pore size should be studied using particles with variety pore sizes.

Future aspects for controlled D-LH_2 release. The original long-range outlook of this D-LH_2 study is to simultaneously load *luciferase-specific inhibitor compounds* (FLICs) into porous silicon nanoparticles with different types of cell *penetrating peptides* (CPPs). Covalent conjugation of FLICs to the particles by a CPP-linkage would enable to study the escape of the particles from the endosomal/lysosomal compartment due to the strong conjugation chemistry which is barely unbroken by endosomal enzymes. (Poutiainen et al. Unpublished manuscript) Later on, the studies could be carried out by Fluc transfected cells and tissues which express constantly FLuc. FLuc transfection provides an opportunity to develop D-LH_2 as an alternative imaging tool for *in vivo* nanoparticle research.

3.5. Conclusion

Mesoporous silicon nanoparticles are widely studied and a versatile tool for drug delivery applications. The aim of the study was to test the drug loading capacity and release kinetics of mesoporous silicon nanoparticles using D-luciferin as a drug like model molecule and use the luciferase catalyzed luminescence reaction for monitoring the kinetics of drug release from the particles. Thermal carbonized porous silicon amino particles (TCPSi-NH_2) were found to have the highest D-LH_2 loading capacity although the attraction seems not be enough for maintaining sustained release. Alternative methods to maintain the D-luciferin inside the mesoporous space are required. In spite of the undesired drug release from TCPSi-NH_2 the method developed here

can be applied for comparing drug loading and release properties of other types of porous silicon nanoparticles. A release test can be carried out easily on a 96 well plate using the drop-by-drop methodology described in this report. In addition, interfering light absorption of porous silicon particles in the bioluminescence release test is also avoidable with the simple and quick dilution procedure. In summary, if the sustained or even eliminated D-LH_2 release to any kind of porous silicon nanoparticles is achieved it would open the doors for developing a new bioluminescence based imaging method for studying drug delivery systems in cellular and even *in vivo* environment.

4. References

Aggarwal G., Mishra P., Joshi B., Harsh S. (2013). Porous silicon surface stability: a comparative study of thermal oxidation techniques. Journal of Porous Materials, 20, 4, 1380-2224.

Anderson S., Elliot H., Wallis D., Canham L., Powell J. (2003). Dissolution of different forms of partially porous silicon wafers under simulated physiological conditions. Physica Status Solidi A, 197, 2, 331-335

Arukuusk P., Pärnaste L., Oskolkov N., Copolovici D., Margus H., Padari K., Möll K., Maslovskaja J., Tegova R., Kivi G., Tover A., Pooga M., Ustav M., Langel U. (2013). New generation of efficient peptide-based vectors, NickFects, for the delivery of nucleic acids. Biochimica et Biophysica Acta, 1828, 5, 1365-1373

Asma A., Dominique D., Jacques B., Vladimir L., Tetyana N., Abdelkader S. (2009). Organization of silicon nanocrystals by localized electrochemical etching. Applied Physics Letters, 95, 15, 1-4.

Bimbo L., Sarparanta M., Santos H., Airaksinen A., Mäkilä E., Laaksonen T., Peltonen L., Lehto V., Hirvonen J., Salonen J. (2010). Biocompatibility of thermally hydrocarbonized porous silicon nanoparticles and their biodistribution in rats. ACS Nano, 6, 4, 3023

Björkqvist M., Salonen J., Laine E., Niinistö L. (2003). Comparison of stabilizing treatments on porous silicon for sensor applications, Physica Status Solidi A - Applications and Materials Science, 2, 197, 374-377

Bley R., Kauzlarich S., Davis J., Lee H. (1996). Characterization of silicon nanoparticles prepared from porous silicon. Chemistry of Materials, 8, 8, 1881-1888

Buriak J., Stewart M., Geders T., Allen M., Choi H., Smith J., Raftery D., Canham L. (1999). Lewis acid mediated hydrosilylation on porous silicon surfaces. Journal of the American Chemical Society, 121, 49, 11491-11502

L. (2000). Porous silicon as a therapeutic biomaterial. Microtechnologies in Medicine and Biology - the 1st Annual International - Conference On. 2000, 109-112

Canham L., Reeves C., Newey J., Houlton M., Cox T., Buriak J., Stewart M. (1999). Derivatized mesoporous silicon with dramatically improved stability in simulated human blood plasma. Advanced Materials, 11, 18, 11, 1505-1507.

Canham L. (1990). Silicon quantum wire array fabrication by electrochemical and chemical dissolution of wafers. Applied Physics Letters, 57, 10, 1046-1048

Canham L. (1996). Bioactive silicon structure fabrication through nanoetching techniques, Advanced Materials, 7, 12, 1033-1037

Canham L., Houlton M., Leong W., Pickering, C., Keen, J. (1991). Atmospheric impregnation of porous silicon at room temperature. Journal of Applied Physics, 70, 1, 422-431

Chen H., Hou X., Li G., Zhang F., Yu M., Wang X. (1996). Passivation of porous silicon by wet thermal oxidation. Journal of Applied Physics, 6, 79, 3282-3285

De Castro C., Mitchell B. (2002). Nanoparticles from mechanical attrition. Synthesis, functionalization and surface treatment of nanoparticles. 1-15, Edited by Marie Isabelle Baraton.

De Villiers M., Otto D., Strydom S., Lvov Y. (2011). Introduction to nanocoatings produced by layer-by-layer (LbL) self-assembly. Advanced Drug Delivery Reviews, 9, 63, 701-715

Dhanekar S., Jain S. (2013). Porous silicon biosensor: current status. 41, 54-64

Ding M., Bowman L., Bowman L., Castranova V. (2012). Luciferase reporter system for studying the effect of nanoparticles on gene expression, Methods in Molecular Biology, 906, 403-414

Drug Bank. (2013). Compound report card - fenofibric acid. available online https://www.ebi.ac.uk/chembl/compound/inspect/CHEMBL981 29.11.2013

EL-Ghany E., Amine A., EL-Sayed A., EL-Kolaly, M., Abdel-Gelil F. (2005). Radiochemical and biological characteristics of radioactive iodine labeled indomethacin for imaging of inflammation, Journal of Radioanalytical and Nuclear Chemistry, 266, 1, 117-124.

Frank M., Fries L. (1991). The role of complement in inflammation and phagocytosis. Immunology Today, 9, 12, 322-326

Gjøen, T., Berg T. (2001). Direct Labelling of Proteins with 125I. Encyclopedia of Life Sciences, 1-7

Hancock B., Parks M. (2000). What is the true solubility advantage for amorphous pharmaceuticals? Pharmaceutical Research, 4, 17, 397-404

He Q., Zhang Z., Gao F., Li Y., Shi J. (2011). In vivo biodistribution and urinary excretion of mesoporous silicon nanoparticles: effects of particle size and PEGylation. Small, 7, 2, 271-280

Heitz F., Morris M., Divita G. (2009). Twenty years of cell-penetrating peptides: from molecular mechanisms to therapeutics. British Journal of Pharmacology, 157, 2, 195-206

Hoebe R., Van D., Stap J., Van Noorden C., Manders E. (2008). Quantitative determination of the reduction of phototoxicity and photobleaching by controlled light exposure microscopy. Royal Microscopical Society, 231, 9-20

Hofmeister H., *Ködderitzsch P., Dutta J.* (1998). Structure of nanometersized silicon particles prepared by various gas phase processes. Journal of Non-Crystalline Solids, 232-234, 182-187

Hu H., Deng H., Fang Y. (2012) Label-Free Phenotypic Profilin Identified D-Luciferin as a PR35 Agonist. Plos One, 4, 7, e34934

Hu Q., Gu G., Liu Z., Jiang M., Kang T., Miao D., Tu Y., Pang Z., Song Q., Yao L., Xia H., Chen H., Jiang X., Gao X., Chen J. (2013). F3 peptide-functionalized PEG-PLA nanoparticles co-administrated with tLyp-1 peptide for anti-glioma drug delivery. Biomaterials, 4, 34, 1135-1145

Huang X., Brazel C. (2001). On the importance and mechanisms of burst release in matrix-controlled drug delivery systems. Journal of Controlled Release, 73, 2-3, 121-136

Huang X., Chen X. (2011). Shape effect of mesoporous silicon nanoparticles on cellular and in vivo functions. Life Science Systems and Applications Workshop, Conference in Bethesda, 73-74

Popplewell J., King S., Day J., Ackrill P., Fifield L., Cresswell R., di Tada M., Liu K. (1998). Kinetics of uptake and elimination of silicic acid by a human subject: A novel application of Si and accelerator mass spectrometry. Journal of Inorganic Biochemistry, 69, 3, 177-180

James, T., Steer A., Musca C., Parish G., Keating A., Faraone L. (2006). Investigation of aging effects in porous silicon. Optoelectronic and Microelectronic Materials and Devices, Conference on 2006, 290-293

Kaasalainen M., Mäkilä E., Riikonen J., Kovalainen M., Järvinen K., Herzig K., Lehto V., Salonen J. (2012). Effect of isotonic solutions and peptide adsorption on zeta potential of porous silicon nanoparticle drug delivery formulations. International Journal of Pharmaceutics, 431, 1, 230-236

Kale P. (2010). Synthesis of si nanoparticles from freestanding porous silicon (ps) film using ultrasonication. Photovoltaic Specialists Conference, 20-25

Kinnari PJ., Hyvönen M., Mäkilä E., Kaasalainen M., Rivinoja A., Salonen J., Hirvonen J., Laakkonen P., Santos H.(2013). Tumour homing peptide-functionalized porous silicon nanovectors for cancer therapy. Biomaterials, 34, 36, 9134-9141

Kovalainen M., Mäkilä E., Salonen J., Lehto V., Herzig K., Järvinen K. (2012). Mesoporous Silicon (PSi) for Sustained Peptide Delivery: Effect of PSi microparticle surface chemistry on peptide YY3-36 release. Pharmaceutical Research, 3, 29, 837-837

Kovalev D. (2004). Photodegradation of porous silicon induced by photogenerated singlet oxygen molecules. Applied Physics Letters, 85, 16, 3590-3592

Kresge C., Leonowicz M., Roth W., Vartuli J., Beck J. (1992). Ordered mesoporous molecular-sieves synthesized by a liquid-crystal template mechanism. Nature, 359, 6397, 710-712

Lai C., Trewyn B., Jeftinija D., Jeftinija K., Xu S., Jeftinija S., Lin V. (2003). A mesoporous silica nanosphere-based carrier system with chemically removable CdS nanoparticle caps for stimuli-responsive controlled release of neurotransmitters and drug molecules. Journal of the American Chemical Society, 125, 15, 4451-4459

Li X., He Y., Swihart M. (2004). Surface functionalization of silicon nanoparticles produced by laser-driven pyrolysis of silane followed by HF-HNO3 etching. Langmuir, 20, 11, 4720-4727

Limnell T. Riikonen J., Salonen J., Kaukonen A., Laitinen L., Hirvonen J., Lehto V. (2007). Surface chemistry and pore size affect carrier properties of mesoporous silicon microparticles. International Journal of Pharmaceutics, 343, 1-2, 141-147

Lipinski C. (2004). Lead- and drug-like compounds: the rule-of-five revolution. Drug Discovery Today: Technologies 1, 4, 337-341

Lipinski C., Lombardo F., Dominy B., Feeney P. (1997). Experimental and computational approaches to estimate solubility and permeability in drug discovery and development settings. Advanced Drug Delivery Reviews, 23, 1-3, 3-25

Low S., Williams K., Canham L., Voelcker N. (2006). Evaluation of mammalian cell adhesion on surface-modified porous silicon. Biomaterials, 27, 26, 4538-4546

Low S., Williams K., Canham L., Voelcker N. (2010). Generation of reactive oxygen species from porous silicon microparticles in cell culture medium. Journal of Biomedical Materials Research Part A, 93, 3, 1124-1131

Mäe M., Myrberg H., El-Andaloussi S., Langel Ü. (2009). Design of a tumor homing cell-penetrating peptide for drug delivery. International Journal of Peptide Research and Therapeutics, 15, 1, 11-15

Mäkilä E., Bimbo L., Kaasalainen M., Herranz B., Airaksinen A., Heinonen M., Kukk E., Hirvonen J., Santos H., Salonen J. (2012). Amine modification of thermally carbonized porous silicon with silane coupling chemistry. Langmuir, 28, 39, 14045-14054

Marques S., Esteves da Silva J. (2009). Firefly bioluminescence: a mechanistic approach of luciferase catalyzed reactions. International Union of Biochemistry and Molecular Biology life Life, 61, 1, 6-17

Mathew, F., Alocilja, E. (2003). Fabrication of porous silicon-based biosensor. Sensors, 1, 293-298

McElroy W. (1951). Properties of the reaction utilizing adenosinetriphosphate for bioluminescence. Journal of Biological Chemistry, 191, 2, 547-557

Nakamura M., Maki S., Amano Y., Ohkita Y., Niwa K., Hirano T., Ohmiya Y., Niwa H. (2005). Firefly luciferase exhibits bimodal action depending on the luciferin chirality. Biochemical and Biophysical Research Communications, 331, 2, 471-475

Nychyporuk, T., Lysenko, V., Gautier, B., Barbier, D. (2006). Silicon nanoparticle formation by short pulse electrochemical etching in the transition regime. Journal of Applied Physics, 100, 10, 1-7

Oskolkov N., Arukuusk P., Copolovici D., Lindberg D., Margus H, Padari K., Pooga M., Langel Ü. (2011). NickFects, phosphorylated derivatives of dransportan 10 for cellular delivery of oligonucleotides. International Journal of Peptide Research and Therapeutics, 17, 2, 147-157

Owens D., Peppas N. (2006). Opsonization, biodistribution, and pharmacokinetics of polymeric nanoparticles. International Journal of Pharmaceutics, 307, 1, 93-102

Pan X., Julian T., Augsburger L. (2008). Increasing the dissolution rate of a low-solubility drug through a crystalline-amorphous transition: a case study with indomethacin. Drug Development and Industrial Pharmacy, 34, 2, 221-231

Park, H., Tsutsumi H., Mihara H. (2013). Cell penetration and cell-selective drug delivery using a-helix peptides conjugated with gold nanoparticles. Biomaterials, 34, 20, 4872-4879

Park, I., Cook S., Kim Y., Kim H., Cho M., Jeong H., Kim E., Nah J., Born H., Cho C. (2005). Glucosylated polyethylenimine as a tumor-targeting gene carrier. Archives of Pharmacal Research, 28, 11, 1302-1310

Park J. Gu L., von Maltzahn G., Ruoslahti E., Bhatia S., Sailor M. (2009). Biodegradable luminescent porous silicon nanoparticles for in vivo applications. Nature Materials, 8, 4, 331-336

Passirani C., Barratt G., Devissaguet J., Labarre D. (1998a). Long-circulating nanoparticles bearing heparin or dextran covalently bound to poly(methyl methacrylate). Pharmaceutical Research, 15, 7, 1046-1050

Petrova-Koch V., Muschik T., Kux A., Meyer B., Koch F., Lehmann V. (1992). Rapid-thermal-oxidized porous Si - The superior photoluminescent Si. Applied Physics Letters, 61, 8, 943-945

Piasek A., Bartoszek A., Namieśnik J. (2009). Phytochemicals that counteract the cardiotoxic side effects of cancer chemotherapy. Postępy Higieny i Medycyny Doświadczalnej, 63, 142-158 (Summary in English), Published Online 17 April 2009, e-ISSN 1732-2693, available http://www.phmd.pl/fulltxt.php?ICID=88332263 29.11.2013

Piepenhagen P., Vanpatten S., Hughes H., Waire J., Murray J., Andrews L., Edmunds T., O'Callaghan M., Thurberg B. (2010). Use of direct fluorescence labeling and confocal microscopy to determine the biodistribution of two protein therapeutics, Cerezyme and Ceredase. Microscopy Research and Technique, 73, 7, 694-703

Poutiainen P., Rönkkö T., Hinkkanen A., Palvimo J., Närvänen A., Turhanen P., Laatikainen R., Weisell J., Pulkkinen J. Firefly Luciferase Inhibitor-conjugated Peptide Quenches Bioluminescence: A Versatile Tool for Real Time Monitoring Cellular Uptake of Biomolecules. Unpublished manuscript

Pubmed Compound. (2004). Compound database, available online: http://pubchem.ncbi.nlm.nih.gov/ 13.1.2014.

Qiu X., Leporatti S., Dontah Möhwald E. (2001). Studies on the drug release properties of polysaccharide multilayers encapsulated inbuprofen microparticles. Langmuir 17, 17, 5375-5380

Raab C., Simkó M., Fiedeler U., Nentwich M., Raab A. (2011). Production of Nanoparticles and Nanomaterials. NanoTrust Dossier no. 6, Published Online February 2011, available http://epub.oeaw.ac.at/ita/nanotrust-dossiers/dossier006en.pdf 29.11.2013.

Rouquerol J., Avnir D., Everett D., Fairbridge C., Haynes M., Pernicone N., Ramsay J., Sing K., Unger K. (1994). Recommendations for the chracterization of porous solids (technical report). Pure and Applied Chemistry, 68, 8, 1739-1758

Royal Society of Chemistry 2013, Ultrasonication. RSC Chemical Methods Ontology, available online http://www.rsc.org/publishing/journals/prospect/ontology.asp?id=CMO:0001708 29.11.2013

Royal Society. (2007) Nanoscience and nanotechnologies: opportunities and uncertainties. The Royal Academic of Engineering. Available Online http://www.nanotec.org.uk/report/Nano %20report %202004 %20fin.pdf 29.11.2013.

Russo L., Colangelo F., Cioffi R., Rea I., Stefano L. (2012). A mechanochemical approach to porous silicon nanoparticles fabrication. Materials 4, 6, 1023-1033

Rytkönen J., Miettinen R., Kaasalainen M., Lehto V., Salonen J., Närvänen A. (2012). Functionalization of mesoporous silica nanoparticles for targeting and bioimaging purposes. Journal of Nanomaterials, 2012, 1-9

Sailor M., (2012). Porous silicon in practice: preparation, characterization and applications. Wiley-VCH Verlag GmbH & Co. KGaA, 1-42, DOI: 10.1002/9783527641901.fmatter

Salonen J. (2013). Homepage of Jarno Salonen - Porous silicon. Available Online http://users.utu.fi/jarsalon/psi.html 17.01.2014

Salonen J., Björkqvist M., Laine E., Niinistö L. (2004). Stabilization of porous silicon surface by thermal decomposition of acetylene. Applied Surface Science, 225, 1-4, 389-394

Salonen J., Kaukonen A., Hirvonen J., Lehto V. (2008). Mesoporous silicon in drug delivery applications, Journal of Pharmaceutical Sciences, 97, 2, 632-653

Salonen J., Laitinen L., Kaukonen A., Tuura J., Björkqvist M., Heikkilä T., Vähä-Heikkilä K., Hirvonen J., Lehto V. (2005). Mesoporous silicon microparticles for oral drug delivery: loading and release of five model drugs. Journal of Controlled Release, 108, 2-3, 362-374

Salonen J., Lehto V. (2008). Fabrication and chemical surface modification of mesoporous silicon for biomedical applications. Chemical Engineering Journal, 137, 1, 162-172

Sarparanta M., Bimbo L., Rytkönen J., Mäkilä E., Laaksonen T., Laaksonen P., Nyman M., Salonen J., Linder M., Hirvonen J., Santos H., Airaksinen A. (2012). Intravenous delivery of hydrophobin-functionalized porous silicon nanoparticles: stability, plasma protein adsorption and biodistribution. Molecular Pharmaceutics, 9, 3, 654-663

Schwartz M., Cunin F., Cheung R., Sailor M. (2005). Chemical modification of silicon surfaces for biological applications. Physica Status Solidi A, 202, 8, 1380-1384

Seliger H., McElroy W., White E., Field G. (1961). Stereospecificity and firefly bioluminescence, a comparison of natural and synthetic luciferins. Proceedings of the *National Academy* of Sciences of the *United States* of America, 47, 8, 1129-1134

Shenoy D., Sukhorukov G. (2004). Engineered microcrystals for direct surface modification with layer-by-layer technique for optimized dissolution, European Journal of Pharmaceutics and Biopharmaceutics, 58, 3, 521-527

Sigma - Aldrich. (2011). Enzymatic assay and ATP sensitivity test of luciferase. Available Online: https://www.safcglobal.com/technical-documents/protocols/biology/enzymatic-assay-of-luciferase.html 29.11.2013

Smith R., Collins S. (1990). Porous silicon morphologies and formation mechanism. Sensors and Actuators A - Physical, 23, 1-3, 825-829

Suh J., Choy K., Lai S., Suk J., Tang B., Prabhu S., Hanes J. (2007). PEGylation of nanoparticles improves their cytoplasmic transport. International Journal of Nanomedicine 2, 4, 735-741

Sun X., Zhao Y., Lin V., Slowing I., Trewyn B. (2011). Luciferase and luciferin co-immobilized mesoporous silica nanoparticle materials for intracellular biocatalysis. Journal of the American Chemical Society, 133, 46, 18554-18557

Tay L., Rowell N., Poitras D., Fraser J., Lockwood D., Boukherroub R. (2004). Bovine serum albumin adsorption on passivated porous silicon layers. Canadian Journal of Chemistry, 82, 10 1545-1553

Thorne N., Inglese J., Auld D. (2010). Illuminating insights into firefly luciferase and other bioluminescent reporters used in chemical biology. Chemistry and Biology, 17, 6, 646-657

Torres-Costa V., Martin-Palma J. (2010). Application of nanostructured porous silicon in the field of optics - a review. 45, 11, 2823-2838

Trewyn B., Slowing I., Giri S., Chen H., Lin V. (2007). Synthesis and functionalization of a mesoporous silica nanoparticle based on the sol-gel process and applications in controlled release. Accounts in Chemical Research, 9, 40, 846-853

Trucks G., Raghavachari K., Higashi G., Chabal Y. (1990). Mechanism of HF etching of silicon surfaces: a theoretical understanding of hydrogen passivation. Physical Review Letters, 65, 4, 504-507

Uhlir A. (1956). Electrolytic shaping of germanium and silicon, Bell System Technical Journal, 35, 2, 333-347

Vallet-Regi M., Ramila A., del Real R., Perez-Pariente J. (2001). A new property of MCM-41: drug delivery system. Chemistry of Materials, 13, 2, 308-311

Varkouhi A. Scholte M., Storm G., Haisma H. (2011). Endosomal escape pathways for delivery of biologicals. Journal of Controlled Release, 151, 3, 220-228

Vazsonyi E., Szilagyi E., Petrik P., Horvath Z., Lohner T., Fried M., Jalsovszky G. (2001). Porous silicon formation by stain etching. Thin Solid Films, 388, 1-2, 295-302

Wang F., Hui H., Barnes T., Barnett C., Prestidge C. (2010). Oxidized mesoporous silicon microparticles for improved oral delivery of poorly soluble drugs. Molecular Pharmaceutics, 7, 1, 227-236

White E., Rapaport E., Hopkins T., Seliger H. (1969). Chemi- and bioluminescence of firefly luciferin. Journal of the American Chemical Society, 91, 8, 2178-2180

Xia B., Xiao S., Wang J., Guo D. (2005). Stability improvement of porous silicon surface structures by grafting polydimethylsiloxane polymer monolayers. Thin Solid Films, 474, 1-2, 306-309

Xu W., Riikonen J., Nissinen T., Suvanto M., Rilla K., Li B., Wang Q., Deng F., Lehto V. (2012). Amine surface modifications and fluorescent labeling of thermally stabilized mesoporous silicon nanoparticles. The Journal of Physical Chemistry C, 116, 42, 22307-22314

Yaakob S., Mohamad A., Ismail J., Noor Hana Hanif A., Ibrahim K. (2012). The formation and morphology of highly doped n-type porous silicon: effect of short etching time at high current density and evidence of simultaneous chemical and electrochemical dissolutions. Journal of Physical Science, 23, 2, 17-31

Yuan W., Fu J., Su K., Ji J. (2010). Self-assembled chitosan/heparin multilayer film as a novel template for in situ synthesis of silver nanoparticles. Colloids and Surfaces B: Biointerfaces, 76, 2, 549-555